

UC Riverside

UC Riverside Electronic Theses and Dissertations

Title

The Development of Warm Gas Cleanup Technologies for the Removal of Sulfur Containing Species from Steam Hydrogasification

Permalink

<https://escholarship.org/uc/item/7mq4v2vb>

Author

Luo, Qian

Publication Date

2012

Peer reviewed|Thesis/dissertation

UNIVERSITY OF CALIFORNIA
RIVERSIDE

The Development of Warm Gas Cleanup Technologies for the Removal of Sulfur
Containing Species from Steam Hydrogasification

A Dissertation submitted in partial satisfaction
of the requirements for the degree of

Doctor of Philosophy

in

Chemical and Environmental Engineering

by

Qian Luo

December 2012

Dissertation Committee:

Dr. Joseph M. Norbeck, Chairperson

Dr. Akua Asa-Awuku

Dr. Sharon Walker

Copyright by
Qian Luo
2012

The Dissertation of Qian Luo is approved:

Committee Chairperson

University of California, Riverside

ACKNOWLEDGEMENTS

I would like to express my sincerest gratitude to my advisor, Professor Joseph M. Norbeck, for his consistent support, warm encouragement, insightful suggestions and scientific guidance during my research. The research turned to be interesting and successful under his instruction. I would also want to acknowledge Dr. Chan S. Park, my co-advisor, who introduced me to the field of warm gas cleanup. I thank him for giving me insightful new ideas about my research. Dr. Kiseok Kim, s professor in Youngnam University, gave me important guidance during my Ph.D. research. I am extremely grateful for his assistance. I express my earnest appreciation to my reading committee members, Professor Sharon Walker, Professor Akua Asa-Awuku and my advance candidacy members, Professor David Kisailus, Professor Jingsong Zhang, for their suggestions. I also wish to thank Junior Castillo, who provided great help in solving mechanical and engineering problems during my experimental setup. I am grateful to my colleagues, Xiaoming Lu, Sangran Hu, Yoothana Thanmongkhon, Amornrat Suemanotham, Wei He, Yang Li and other graduate students in our lab. They offered many valuable suggestion and useful discussions. I warmly thank Kurt Bumiller, for useful suggestions for my experimental setup and in the operation of analytical equipment. I want to give my special thanks to my parents, my older sister, my uncle and my grandfather. Their endless love helped me overcome a lot of difficulties I met in my life. This study would not have been completed without their love and support.

Qian Luo

ABSTRACT OF THE DISSERTATION

The Development of Warm Gas Cleanup Technologies for the Removal of Sulfur
Containing Species from Steam Hydrogasification

by

Qian Luo

Doctor of Philosophy, Graduate Program in Chemical and Environmental Engineering
University of California, Riverside, December 2012
Dr. Joseph M. Norbeck, Chairperson

The steam hydrogasification reaction (SHR) refers to the thermochemical conversion of carbonaceous materials into synthetic gas in a steam and hydrogen environment. The formation of gaseous sulfur species from the solid sulfur in the feedstock is commonplace in thermochemical processes. It requires the cleaning of the output gas to protect the operation of downstream processes and catalysts. This thesis presents the results of an experimental study to determine the effect of temperature, steam and H_2 partial pressure has on the distribution of the various gaseous sulfur species in the outlet gas of the SHR. Experiment results showed that sulfur in the feedstock is mainly converted to H_2S in the SHR process. COS and CS_2 were undetectable. The H_2 and steam rich environment in the SHR process is favorable for the formation of H_2S and suppresses the COS and CS_2 formation. An increase of H_2S concentration was observed with the rise in temperature from $700^\circ C$ to $800^\circ C$. An increase in the partial pressure of H_2 decreased the H_2S concentration released in the gas phase.

A lab-scale warm gas cleanup system was developed using commercial ZnO sorbents based on our preliminary results and literature search. A mixture gas simulated

the composition of syngas from steam hydrogasification reaction and was used as the feed gas. The effect of space velocity and gas composition on H₂S breakthrough time was studied. It was found that H₂S breakthrough time and sulfur capture capacity increased as the space velocity decreased. Moreover, addition of H₂ or CH₄ to the inlet gas stream has the positive effect on H₂S breakthrough time. Addition of CO to the inlet gas stream decreased H₂S breakthrough time. The addition of low concentration of CO₂ to the inlet gas stream had little influence on H₂S breakthrough time.

Techno-economic analysis was performed based on experimental and Aspen Plus simulation results in order to design warm gas cleanup system for the CE-CERT process. It was found that a warm gas cleanup process using regenerable sorbent is preferred for a high capacity plant (syngas feed ≥ 1000 tonne/day). And, a warm gas cleanup process using disposable sorbent is more feasible for low capacity plant (syngas feed < 1000 tonne/day). Economic sensitivity results showed that H₂ availability and price is the most influential parameter affecting the cost for a warm gas cleanup process using regenerable sorbent, while ZnO sorbent price is the most influential parameters affecting the cost for warm gas cleanup process by using disposable sorbent.

Table of Contents

Chapter 1 Introduction	1
1.1 Background	1
1.1.1 Gasification	2
1.1.2 Pyrolysis.....	4
1.1.3 Combustion	6
1.1.4 Liquefaction	6
1.2 Introduction of the CE-CERT Process.....	7
1.3 Gas Cleanup Requirement	10
1.4 Thesis Objective.....	12
References	14
Chapter 2 Formation of Gaseous Sulfur Species in Steam Hydrogasification Reaction ...	17
2.1 Introduction.....	17
2.1.1 Sulfur in the Feedstock	17
2.1.2 Formation of Sulfur Pollutants during Gasification Process	19
2.2 Simulation Work.....	25
2.2.1 Aspen Simulation.....	25
2.2.2 Aspen Simulation Results	26
2.3 Experimental Section	27
2.3.1 Materials	27
2.3.2 Apparatus	28
2.3.3 Experimental Procedure.....	30

2.4 Experimental Result and Discussion.....	32
2.4.1 Sulfur Formation in the Gas Phase	32
2.4.2 Effect of Temperature	33
2.4.3 Effect of Steam (Water).....	35
2.4.4 Effect of H ₂ Partial Pressure	37
2.5 Conclusion	38
References	40
Chapter 3 Hydrogen Sulfide Removal from Syngas Produced by Steam Hydrogasification	
Reaction	43
3.1 Desulfurization Technologies	43
3.1.1 Selexol Scrubbing	43
3.1.2 Warm Gas Cleanup	44
3.2 Metal Oxide Sorbents Screening.....	45
3.2.1 Copper Oxide Based Sorbents	48
3.2.2 Iron Oxides Based Sorbents.....	48
3.2.3 Manganese Oxide Based Sorbents.....	49
3.2.4 Zinc Oxide Based Sorbents.....	50
3.2.5 Reaction Schemes	51
3.3 Experimental Setup and Analytic Methods	53
3.3.1 Sorbent	53
3.3.2 Desulfurization Setup.....	54
3.3.3 Flow Rate Control.....	56

3.3.4 Steam Generation.....	57
3.3.5 GC Calibration.....	57
3.3.6 Experimental Procedure.....	58
3.4 Result and Discussion.....	59
3.4.1 Effect of Space Velocity on H ₂ S Adsorption.....	59
3.4.2 Effect of Gas Composition on H ₂ S Adsorption.....	61
3.4.2.1 Addition of H ₂ in Inlet Gas Stream.....	65
3.4.2.2 Addition of CH ₄ to the Inlet Gas Stream.....	67
3.4.2.3 Addition of CO to the Inlet Gas Stream.....	68
3.4.2.4 Addition of CO ₂ to the Inlet Gas Stream.....	70
3.5 Conclusion.....	71
References.....	73
Chapter 4 Techno-economic Evaluation for Gas Cleanup System for CE-CERT Process	77
4.1 Introduction.....	77
4.1.1 Reactor and System.....	79
4.1.1.1 Fixed-Bed Reactor.....	79
4.1.1.2 Moving Bed Reactor.....	81
4.1.1.3 Fluidized Bed.....	83
4.2 Economical Analysis of H ₂ S Removal by Using Regenerable Sorbent.....	85
4.2.1 Process Description.....	85
4.2.2 Aspen Simulation Flow Chart.....	87
4.3 Economical Analysis of H ₂ S Removal by Using Disposable Sorbent.....	90

4.3.1 Process Description.....	90
4.3.2 Economical Analysis	90
4.4. Results	91
4.4.1 Annual Operation Cost and Net Present Value (NPV)	91
4.4.2 Economic Sensitivity Studies	94
4.5 Conclusion	100
References	101
Chapter 5 Conclusions and Future Work	103
Appendices.....	106

List of Tables

Table 2.1 Syngas impurities and tolerances for Fischer-Tropsch and steam methane reforming.....	Error! Bookmark not defined.
Table 2.1 Sulfur level of different feedstock	17
Table 2.2 A summary of possible inorganic reaction involving sulfur compounds during gasification and pyrolysis process	20
Table 2.3 A summary of possible organic reaction involving sulfur compounds during gasification and pyrolysis process	21
Table 2.4. Proximate and ultimate analysis of the coal sample	28
Table 3.1 Properties of zinc oxide sorbent.....	53
Table 4.1 Sensitivity parameters for warm gas cleanup using disposable sorbent	95
Table 4.2 Sensitivity parameters for warm gas cleanup using regenerable sorbent	95

List of Figures

Figure 1.1 Gasification process	4
Figure 1.2 Flow diagram of the CE-CERT process	9
Figure 2.1 Coal forms of sulfur in coal (R and R' are organic C _x H _y group)	19
Figure 2.2 H ₂ O/C mass Ratio vs H ₂ S mass flow rate at different temperature.....	26
Figure 2.3 H ₂ O/Coal mass ratio vs COS mass flow rate at different temperature.....	26
Figure 2.4 H ₂ O/Coal mass ratio vs CS ₂ mass flow rate at different temperature	27
Figure 2.5 Schematic diagram of the stirred batch reactor	29
Figure 2.6 Photograph of the stirred batch reactor setup	30
Figure 2.7 The effect of water to coal mass ratio on H ₂ S concentration at different temperature	33
Figure 2.8 The effect of the water to coal mass ratio on the mass of sulfur in the gas phase at different temperature.....	35
Figure 2.9 The effect of water to coal mass ratio on H ₂ S concentrations at different temperature	36
Figure 2.10 The effect of water to coal mass ratio on the mass of sulfur in the gas phase at different temperature.....	37
Figure 2.11 H ₂ partial pressure effect on the mass of sulfur in the gas phase at 800°C	38
Figure 3.1 Conventional Selexol process for removal H ₂ S from syngas.....	44
Figure 3.4 Scheme of reaction between ZnO and H ₂ S in H ₂ S-H ₂ -CO ₂ -H ₂ O-CO ₂ -N ₂	51
Figure 3.5 Schematic diagram of the experimental apparatus	55
Figure 3.6 Reactor used in desulfurization system	56

Figure 3.7 Relationship between the square root of FPD peak area and H ₂ S concentration	57
Figure 3.8 Effect of space velocity on H ₂ S breakthrough time	60
Figure 3.9 Effect of space velocity on H ₂ S on sulfur capture capacity for H ₂ S breakthrough	61
Figure 3.10 Effect of gas composition on H ₂ S breakthrough time with 6000 h ⁻¹ space velocity	62
Figure 3.11 Effect of gas composition on H ₂ S breakthrough time with 12000 h ⁻¹ space velocity	63
Figure 3.12 Effect of gas composition on H ₂ S breakthrough time with 24000 h ⁻¹ space ..	64
Figure 3.12 Effect of H ₂ on H ₂ S breakthrough time	65
Figure 3.13 Effect of CH ₄ on H ₂ S breakthrough time	67
Figure 3.14 Effect of CO on H ₂ S breakthrough time.....	68
Figure 3.15 Effect of CO ₂ on H ₂ S breakthrough time	70
Figure 4.1 Schematic of fixed-bed reactor.....	81
Figure 4.2 Schematic of moving-bed reactor.....	83
Figure 4.3 Schematic of fluidized-bed reactor.....	85
Figure 4.4 Schematic of H ₂ S removal process by using regenerable ZnO sorbent	86
Figure 4.5 Aspen Plus simulation process flow diagram from the Aspen Plus user interface.....	88
Figure 4.6 Schematic diagram of a fixed-bed reactor process for H ₂ S removal by using disposable sorbent.....	91

Figure 4.7 Operation cost as a function of syngas feed	93
Figure 4.8 NPV as a function of syngas feed.....	93
Figure 4.9 Sensitivity results for warm gas cleanup by using disposable sorbent.....	96
Figure 4.10 Sensitivity results for warm gas cleanup by using disposable sorbent.....	97
Figure 4.11 Sensitivity results for warm gas cleanup by using regenerable sorbent.....	98
Figure 4.12 Sensitivity results for warm gas cleanup by using regenerable sorbent	99

Chapter 1 Introduction

1.1 Background

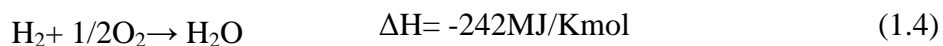
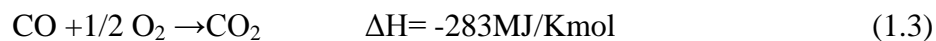
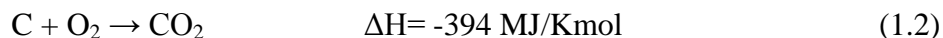
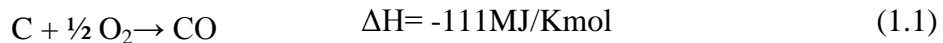
Carbonaceous materials, e.g. coal, biomass (forest and agricultural residues, urban wood wastes, and dedicated energy crops), municipal solid wastes and industrial residues, have the potential to provide alternative pathways to provide energy on a global scale [1]. However, there are concerns of the emissions from the use of some of these materials related to either greenhouse gas emissions and/or criteria pollutants from their burning [2]. The need to control and treat air pollution has been an environmental and health-related concern for several decades. The pollutants include, in part, volatile organic compounds (VOC) that participate in the formation of smog, particulate matter associated with numerous health problems and urban visibility and nitric and sulfur oxides resulting in acid deposition. We are continually challenged to develop new technologies (via physical, chemical and biological methods) for converting carbonaceous materials to clean energy and fuels and chemicals. Conversion of carbonaceous materials may be conducted via two major pathways; thermo-chemical (gasification, liquefaction and pyrolysis) and biological methods (bacterial, enzymatic, et.al) [3].

Thermo-chemical pathways for alternative fuel production generally utilize either gasification or pyrolysis technologies. A literature review of thermo-chemical technologies is presented in the next section.

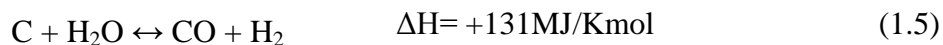
1.1.1 Gasification

Gasification is the conversion of carbonaceous materials to combustible gases consisting of carbon monoxide (CO), hydrogen (H₂) and methane (CH₄) by heating in a gasification medium such as air, oxygen or steam [4] (as showed in Figure 1.1). This mixture gas is called producer gas or syngas. Producer gas can be used to run internal combustion engines (both compression and spark ignition), or used as substitute for furnace oil in direct heat applications and can be used to produce, in an economically viable way, methanol – an extremely attractive chemical which is useful both as fuel for heat engines as well as chemical feedstock for industries [5]. In gasification process, basic chemical reactions were summarized from 1.1 through 1.9 [6, 7]

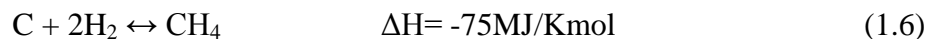
Combustion reactions:



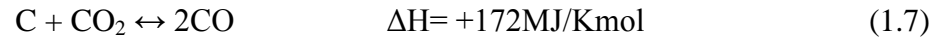
Water gas reaction:



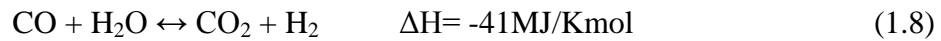
Methanation reaction:



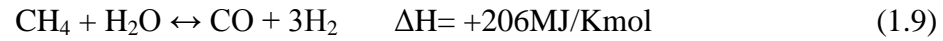
Boudouard reaction:



CO shift reaction:



Steam methane reforming reaction:



In the reactions above, a positive entropy value means an endothermic reaction and a negative entropy value means an exothermic reaction. Moreover, reactions 1.1 to 1.5 are irreversible while reactions 1.6 to 1.9 are incomplete and reversible.

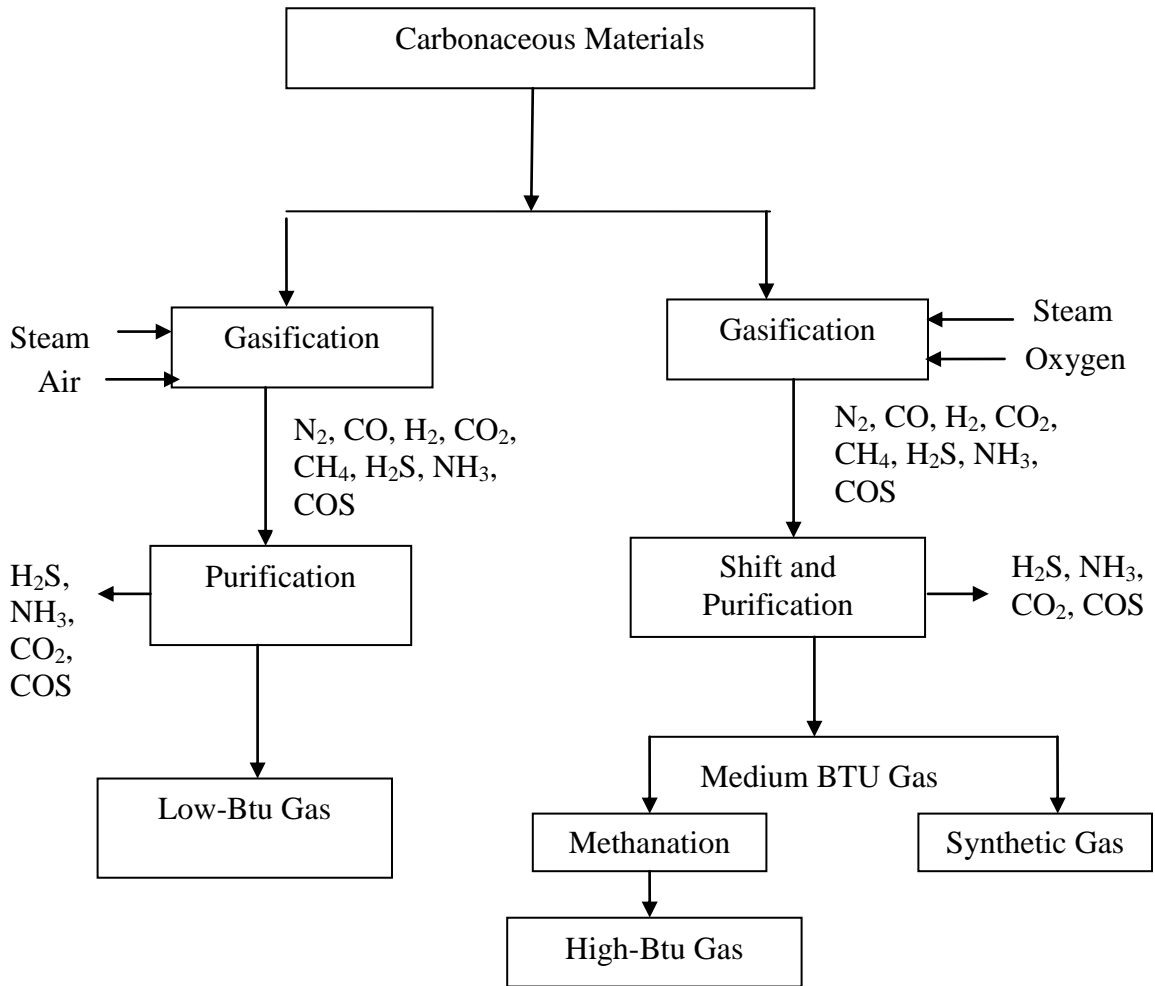


Figure 1.1 Gasification process

As the use of oxygen for gasification is expensive, air is normally used as gasification agent. The disadvantage of gasification is that the nitrogen introduced with the air dilutes the product gas, giving low btu-gas [8].

1.1.2 Pyrolysis

Pyrolysis and gasification also involves thermal decomposition, but pyrolysis is done at somewhat lower temperatures, and in the absence of oxygen. Pyrolysis takes

place at a temperature range of 200 °C to 550 °C depending on the feedstock properties and technological requirements [9].

Pyrolysis is an endothermic process, which needs heat to cause the decomposition to occur. There is another process in presence of hydrogen and it is called hydrolysis. This process is exothermic and reduces the need for heat [10].

The outputs of pyrolysis are carbon char (which can be almost pure carbon), a highly combustible hydrocarbon gas, consisting mainly of carbon monoxide, hydrogen, methane and alkenes; and distillate oil. Composition of the output of pyrolysis is greatly dependent upon the type of material to be processed, the amount of moisture present and the size and density of that material [11].

Changing the conditions of a pyrolysis process will also yield different results. Altering the temperature, pressure and speed at which a reaction takes place will result in different quantities of each residual and potentially shift the energy balance among each of them [11]. During a fast pyrolysis process, for example, the main product, bio-oil, resulted from rapid cooling of the pyrolysis vapors. It becomes a miscible mixture of polar organics (about 75%-80%) and water (about 20%-25%). Yields are up to 80 wt% in total (wet basis) from dry carbonaceous feed with some by-product char and gas [12].

Major challenges for pyrolysis include cleanup of the bio-oil and sufficient stabilization of it for practical delivery and use in a petroleum refinery [9].

1.1.3 Combustion

Combustion can be defined as a series of free radical reactions whereby carbon and hydrogen in the feedstock react with oxygen to form CO₂ and H₂O while liberating useful heat according to the following reaction from Reaction 1.10-1.12 [13].



Oxygen is supplied in excess to ensure complete combustion of the fuel. Thus, production on CO is minimized while the heat release is maximized. The flue gas does not have any residual heating value [13]. The advantage of combustion process is that direct combustion employs well-developed, commercially-available technology. However, the disadvantage of combustion includes low efficiency associated with burning high moisture feedstock, agglomeration and ash fouling due to alkali compounds of some feedstock such as biomass, relatively low thermodynamic efficiencies for steam power plants of the size appropriate to power [14].

1.1.4 Liquefaction

Liquefaction is an industrial process in which coal or biomass as input material is converted into liquid hydrocarbon mixtures; which under further processing becomes desired liquid fuels or chemical feedstock [15]. Liquefaction process is classified into two categories: direct liquefaction and indirect liquefaction [15]. In direct liquefaction, fuels are produced in a process similar to hydrocracking of heavy oils in current refineries. Hydrogen is added to the carbon chain, heteroatoms are removed, and the larger

molecules are cracked and rehydrated to clean fuel molecules at energy efficiency over 75% [16]. In indirect liquefaction process, fuels and chemicals are constructed from single carbon structures (syngas) produced by gasification into higher molecular weight fuels by Fischer-Tropsch reaction. Indirect liquefaction processes have low thermal efficiency, of the order 40–45% [17].

In liquefaction process, liquid yield is high. However, some issues like low product quality, high temperatures and pressures daunt industrial applications of this process [18].

1.2 Introduction of the CE-CERT Process

The College of Engineering Center for Environmental Research and Technology (CE-CERT) at the University of California, Riverside (UCR) is developing a multi-step thermal chemical process called steam hydrogasification (SHR) which has been shown to convert carbonaceous feedstock into syngas (H_2 and CO mixture) with high conversion and potentially a cost effective manner. SHR is the hydrogasification reaction with the addition of steam. Through a series of research projects conducted at CE-CERT, it has been found that SHR increases the rate of formation of methane up to 13 times compared to conventional dry hydrogasification. It is believed that the superheated steam enhances the decomposition of the carbon containing compounds and provides a highly porous solid surface that enhances the reactivity with hydrogen [19, 20].

The CE-CERT process is an integrated system of three steps, as shown in Figure 1.2. The SHR step is followed by the SMR (Steam Methane Reforming) step and a final step of liquid fuel synthesis like a Fischer-Tropsch reactor (FTR). The SHR step utilizes a

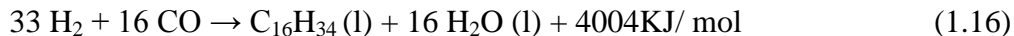
water-based slurry as the source of carbonaceous feedstock and combines it with steam and recycled hydrogen to produce a methane rich gas. The exothermic SHR of the carbonaceous feedstock in slurry can be represented chemically in a simplified manner as:



After the SHR, a warm gas clean up step is used to decrease pollutants including sulfur compounds, ammonia and “tars” (a mix of loosely defined organic condensable compounds) to the level that can simultaneously comply with environmental regulations and also protect any catalysts used in downstream processing. The SMR converts products formed in reaction (1.13) into synthesis gas and can be characterized as:



The reformed syngas comprises of H₂ and CO with a specific ratio dependent on the initial H₂O to C ratio input to the SHR. This syngas ratio is usually optimized for a Fischer-Tropsch Reaction (FTR) by separating and recycling of excess H₂ back into SHR. An internal, self-sustaining source of H₂ can be achieved between the SHR and SMR, such that no external H₂ source is required [18, 19]. Thus, the overall reaction sequence can be characterized by the following equation:



The system has been shown to be self-sustaining provided the output from the SMR is

$$2.06 \leq [H_2 / CO] \leq 2.3$$

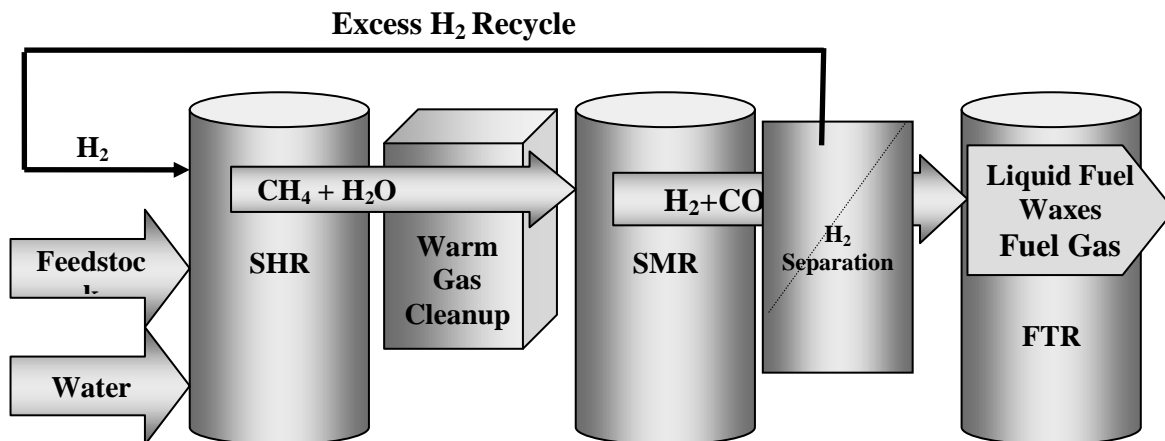


Figure 1.2 Flow diagram of the CE-CERT process

The technical advantages of the CE-CERT process are summarized as follows:

1. It utilizes a slurry feed, so wet feedstocks can be used which reduces cost of drying the feedstock and offers the potential of more efficient handling of feedstock;
2. It entails a closed-loop H₂ cycle and is operated without external H₂ supply;
3. It provides a high rate of methane which could be used as a source of clean synthetic natural gas;
4. It operates under reductive conditions; hence no external O₂ supply is required.
5. It operates under relatively lower temperature and lower pressure compared with other gasification processes (e.g. Partial Oxidation) and offers versatility for both small scale and large scale applications;
6. The optimum H₂ to CO ratio for efficient downstream production of fuel products and chemicals can be achieved by controlling the initial H₂O to C ratio input to the SHR.

One of the byproducts of reaction (1.13) are various sulfur compounds whose concentrations from the SHR depends on the sulfur level in the feedstock and the type

and conditions of the gasifier design. This is of considerable importance and has received considerable of attention. The concern for poisoning (deactivation) is the Ni based steam methane reforming catalyst, and the Fischer-Tropsch catalyst (either Fe or Co) in the following step. Thus, a gas clean up system must remove sulfur and other contaminants to a sufficiently low level to ensure high efficiency operation and lifetime for both reactors.

1.3 Gas Cleanup Requirement

The syngas produced from gasification processes can be burned to produce heat, coupled to gas turbines or fuel cells to produce electrical power or used for the synthesis of hydrogen methanol, and liquid fuels [21]. Sulfur contaminants in the syngas are of great concern due to environmental issues with release to the atmosphere and the detrimental effects on downstream catalysts [22].

Sulfur, mostly as gaseous hydrogen sulfide (H_2S), is considered as a primary poison, seriously deactivating the catalysts used for downstream unit operations such as steam-methane reforming or Fischer-Tropsch synthesis [23]. Conventional steam reforming catalysts are 10-33 wt.% NiO on a mineral support (alumina, cement, or magnesia). The high temperature shift (HTS) catalyst has an iron oxide, chromium oxide basis while the major component in the low temperature shift (LTS) catalyst is copper oxide, usually in a mixture with zinc oxide [24].

Exposure of a nickel surface to gas streams containing as low as 1ppmv H_2S results in surface Ni_xS_y phases leads to a decrease of surface Ni available [21].



Sulfur actually reconstructs the nickel surface preventing or modifying further adsorption of reactant molecules. The LTS catalyst is very sensitive to sulfur. HTS catalysts can tolerate sulfur concentrations up to several hundred ppm, although the activity will decline. The sulfur concentration in the reformer feed gas should be less than 0.5 ppm to maintain a 3-year catalyst lifetime. Uranium oxide and chromium oxide are used as a promoter in certain reforming catalysts resulting in a higher tolerance to sulfur poisoning [24].

The Fischer-Tropsch synthesis (FTS) catalysts are poisoned by sulfur. Sulfur compounds rapidly deactivate both iron and cobalt catalyst presumably by forming surface metal sulfides that do not have FTS activity. Fischer recommended 4 ppm as the maximum sulfur content in the FTS feed gas. Dry recommends a maximum sulfur content of 0.2 ppm based on commercial experience in the Sasol plants [25]. Co catalysts are more sensitive to sulfur poisoning than Fe catalysts. Given the relative cost of Co versus Fe, more efficient sulfur removal should be expected for FTS with Co catalysts. Several more recent references cite even lower sulfur tolerances. Boerrigter, et al report that sulfur levels in syngas for FTS should be below 1 ppm [26] and Turk, et al. claim that the total sulfur content in syngas should be 60 ppb [27]. In general, for a fixed bed reactor any catalyst poison will have the most pronounced affect near the gas inlet and propagate through the reactor towards the outlet, whereas in a fluidized bed design the poison will have a uniform affect throughout the reactor. There is really no safe sulfur level in FTS. And the level of gas cleaning required is based on economic considerations; namely how

long the catalyst remains active versus the investment in gas cleaning [24]. Requirement for level of sulfur was summarized in Table 1.1.

Table 1.1 Syngas impurities and tolerances for Fischer-Tropsch and steam methane reforming

Process	Contaminant	Level	Source
		0.2ppm	[25]
Fischer-Tropach Synthesis	Sulfur	1 ppm	[26]
		60 ppb	[27]
		<0.5ppm for reformer Catalyst life for 3	
Steam Methane Reforming	Sulfur	years	

1.4 Thesis Objective

The overall goal of this thesis is to develop an efficient, economically and technically viable warm gas sulfur removal technology that can be used with the steam hydrogasification reaction process. This will involve the following technical objectives at investigating sulfur distribution in CE-CERT Steam Hydrogasification and developing warm gas cleanup process for CE-CERT Process. The following objectives will be accomplished as part of the research effort.

1. The first objective of the thesis is to investigate the chemical conversion of sulfur species during the SHR process. Coal will be used as the feedstock. A mini batch reactor will be used to simulate the SMR reaction process. Quantitative analysis of the

gaseous sulfur species as well as the solid and liquid residue will be performed to ensure a full mass balance of the entire sulfur in the feed. The impact of the major process variables such as temperature, feedstock composition and pressure on the formation or distribution of gaseous sulfur species will be investigated. The quantification of the expected sulfur species, such as carbonyl sulfide (COS), carbon disulfide (CS₂) and hydrogen sulfide (H₂S) will be performed with a Gas Chromatograph (GC) equipped with Flame Photometric Detector (FPD). The simulation of the SHR process using ASPEN will be used to assist with predicting sulfur species and expected concentrations during steam hydrogasification. Carbon conversion will be determined for all experiments.

2. Metal oxide sorbents will be selected based on the optimal sulfur capture capacity under CE-CERT operating condition with the main focus on H₂S removal. The effect of syngas composition including CH₄, CO, CO₂ and H₂ and space velocity on desulphurization efficiency will be explored and documented.

3. The third objective of this thesis is to do tech-economic analysis for warm gas cleanup of CE-CEERT process. Sulfur can be removed either by disposable sorbent and regenerable sorbent. During warm gas cleanup process by using regenerable sorbent, sulfur removed from syngas can be converted to SO₂ during sorbent regeneration process. A direct sulfur recovery process (DSRP) is necessary to be developed for prevention the SO₂ from being discharged to the environment. A technically and economic feasibility study of two types of warm gas cleanup process will be completed based on experiment results and ASPEN simulation results.

References

1. A. Demirbas, Biomass resource facilities and biomass conversion processing for fuels and chemicals, *Energy Conversion & Management*, 2001, 42(11), 1357-1378.
2. R. Bailie, Current Developments and problems in biomass gasification sixth annual meeting biomass energy institute, Winnipeg, Manitoba, Canada, October, 1977.
3. E. Kan, M. A. Deshusses, Development of foamed emulsion bioreactor for air pollution control, *Biotechnology and Bioengineering*, 2003, 84(2), 240–244.
4. S.K. Hoekman, Biofuels in the U.S. – challenges and opportunities, *Renewable Energy*, 2009, 34(1), 14-22.
5. X. Sha, Coal gasification. Coal, oil shale, natural bitumen, heavy oil and peat-Vol.I.
6. T.B. Reed, Graboski, M., and Markson, M., The SERI High Pressure Oxygen Gasifier, Report SERI/TP-234-1455R, Solar Energy Research Institute, Golden, Colorado, Feb, 1982.
7. C. Higman, M. Burgt, Gasification. 2003. Elsevier/Gulf Professional Pub.
8. R.H Perry, D.W. Green, Perry's chemical engineers handbook. 2008: McGraw-Hill.
9. P. McKendr. Energy production from biomass (part 3): gasification technologies. Bioresource Technology.
10. S.K. Hoekman, Biofuels in the U.S. – challenges and opportunities, *Renewable Energy*, 2009, 34(1), 14-22.
11. P. Dominov, R. Gilyazetdinova, B. Zhirnov, I. Tarasov, R. Khlestkin. Overview world technologies of pyrolysis and perspective of development.UDC 665.6/.7.
12. http://www.biomassinnovation.ca/pdf/factsheet_GPSP_Pyrolysis.pdf
13. A.V. Bridgwater, D. Meier, D. Radlein, An overview of fast pyrolysis of biomass, *Organic Geochemistry*, 1999, 30 (12), 1479-1493.
14. http://www soi.wide.ad.jp/class/20070041/slides/04/index_46.html

15. http://fyi.uwex.edu/mrec/files/2011/04/2005_PowerViaGasification.pdf
16. A.G. Comolli, P. Ganguli, R.H. Stalzer, The direct liquefaction co-processing of coal, oil, plastics, MSW and biomass. Hydrocarbon Technologies, Inc.
17. <http://www.scribd.com/doc/51662168/104/Indirect-liquefaction>.
18. N. Amin, J. Akhtar, S. Kuang. Product of characterization from catalytic liquefaction of empty palm fruit bunch (EPFB) in water and supercritical water.
19. S.K. Raju, S.P Chan, J. M Norbeck, Steam hydrogasification of coal-wood mixtures in a batch reactor, in International Pittsburgh Coal Conference 2008. 2008: Pittsburgh, PA, USA.
20. S.K. Jeon, et al., Characteristics of steam hydrogasification of wood using a micro-batch reactor. *Fuel*, 2007, 86(17-18), 2817-2823.
21. W Torres, S. S. Pansare, J. G. Goodwin. Hot gas removal of tars ammonia and hydrogen sulfide from biomass gasification gas. *Catalysis Review*, 2007, 49(4), 407-456.
22. H. Kuramochi, W Wei, K. Kawamoto, Prediction of the behaviors of H₂S and HCl during gasification of selected residual biomass fuels by equilibrium calculation, *Fuel*, 2005, 84(4), 377-387.
23. J. Koningen et al., Sulfur-deactivated steam reforming of gasified biomass. *Ind.Eng. Chem. Res.* 1998, 37(2), 341.
24. P.L. Spath and D.C. Dayton, Preliminary screening—technical and economic assessment of synthesis gas to fuels and chemicals with emphasis on the potential for biomass-derived syngas. National Renewable Energy Laboratory, NREL/TP-510-34929, December, 2003.
25. M.E Dry, The Fischer-Tropsch synthesis. *Catalysis, Science and Technology*, (J.R. Anderson, M. Boudart, eds.), Springer-Verlag, Vol. 1, 159-256.
26. H. Boerrigter, H.den Uil and H.P Calis. (2002). Green diesel from biomass via Fischer-Tropsch synthesis: new insights in gas cleaning and process design. Paper presented a Pyrolysis and Gasification of Biomass and waste, Expert Meeting, 30 September, 2002, Strasbourg, FR.

27. B.S Turk, et al. Novel technologies for gaseous contaminants control. Final Report for DOE Contract No. DE-AC26-99FT40675, September 2001.

Chapter 2 Formation of Gaseous Sulfur Species in Steam Hydrogasification Reaction

2.1 Introduction

2.1.1 Sulfur in the Feedstock

The sulfur level in potential feedstocks varies greatly. Table 2.1 summarizes sulfur level of different feedstock [1-3].

Table 2.1 Sulfur level of different feedstock

Feedstock	Sulfur (Wt. %)	Feedstock	Sulfur (Wt.%)
Sawdust	0.01	Cedar wood	0.02
Urban wood waste	0.07	Bagasse	0.05
Switchgrass	0.16	Rice straw	0.06
Alfalfa stalks	0.09	Animal manure	1.45
Peat	0.2	Dried sludge ^(C,B,L)	0.66,1.33,0.45
Hunt coal	0.61	China coal ^a	0.17
Arizona Coal	0.49	Illinois coal ^a	3.26

a: analysis provided by Huffman Laboratory. C, B, L :wastewater treatment plant in De la Selva, Banyoles-Terri(B), and Lloret de Mar(L) in Spain[1-3]

Notice that the sulfur levels in biomass and sludge are considerable lower when compared to various forms of coal. Therefore, removal of sulfur in coal has received much more attention. Coal represents a mixture of carbonaceous organic matter, inorganic matter, mineral matter and moisture. The chemical composition is composed of the elements such as carbon, hydrogen, oxygen, sulfur, nitrogen and in trace quantities, phosphorous and some metals. The relative concentration of the above elements depends

strictly on a coal rank (The rank of coal is the stage the coal has reached on the coalification path) .There is an increase in carbon content and a decrease in moisture content and volatile matter with increasing rank [4].

The mineral matter of coal is a heterogeneous mixture of various compounds, some of which is associated chemically with the organic matter. The major components of mineral matter are silicates, aluminosilicates, carbonates, sulfates, and sulfides. Sulfur is chemically integrated throughout coal. It is contained in the organic matter as well as in the mineral matter. Thus, sulfur is present in three basic chemical forms: organic, inorganic and elementary sulfur [5]. The total sulfur in coal varies in the range of 0.2-11 wt%, but in most cases is between 1 and 3 percent by weight [6]. Traditionally, the sulfur compounds have been classified into two groups, inorganic and organic. Organic sulfur is that which is bound to the hydrocarbon structure of the coal. Inorganic sulfur is the remainder [7]. Only divalent organic sulfur is present in coal. This sulfur is present in the form of various organic sulfur groups whose reactivity varies widely. The structure of the organic radical which is connected to the sulfur atom has deterministic effect on the rate of the reaction of the sulfur group. In the class of organic sulfur, two types of compounds were distinguished: the disulphides and the sulphates. Most of the sulfur is in the form of FeS_2 . The sulfur form in coal is showed in Figure 2.1 [6].

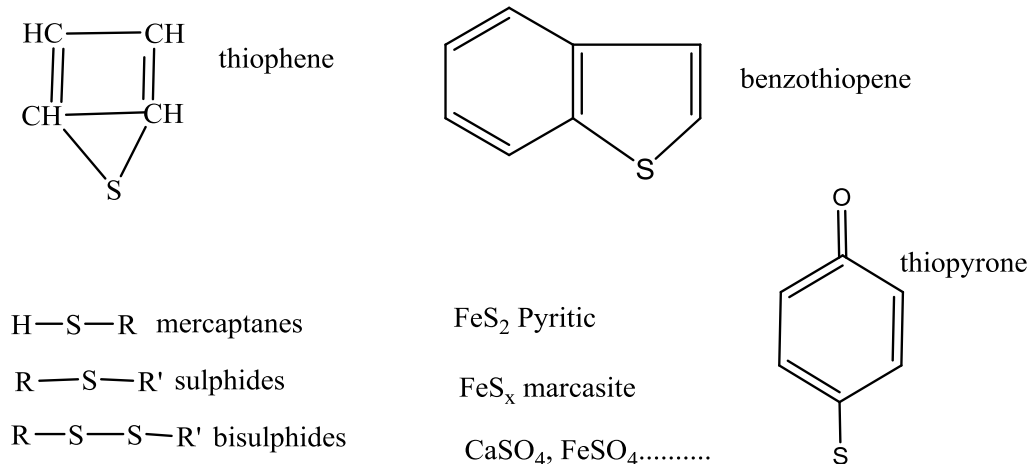


Figure 2.1 Coal forms of sulfur in coal (R and R' are organic C_xH_y group)

2.1.2 Formation of Sulfur Pollutants during Gasification Process

The reactions of sulfur during coal thermal-chemical methods have been received a lot of attention. The reactions are summarized in Table 2.2 and Table 2.3 [7].

During pyrolysis process, the sulfur compounds present in coal are decomposed by temperature and can participate in reactions with the other products of coal pyrolysis. As a result, a portion of the sulfur remains in the coke, while the rest passes into the tar and gas. The primary volatile sulfur reacts further with coal organic matter, or is subject to reactions in the gaseous phase [8].

The behavior of sulfur compounds during coal pyrolysis is determined by many factors including properties of the coal (rank of coal, petrographic structure, mineral matter content, sulfur content and its forms), the parameters of the process (temperature, pressure, reaction time, size distribution of pyrolysed coal) [9] and other factors such as heating rate, time, pressure and velocity of the carrying gas, type of reactor, etc. [10].

Table 2.2 A summary of possible inorganic reaction involving sulfur compounds during gasification and pyrolysis process

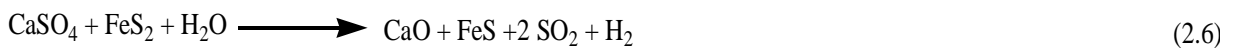
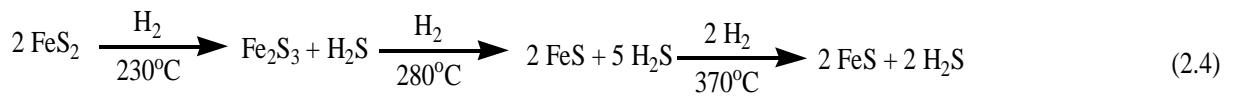
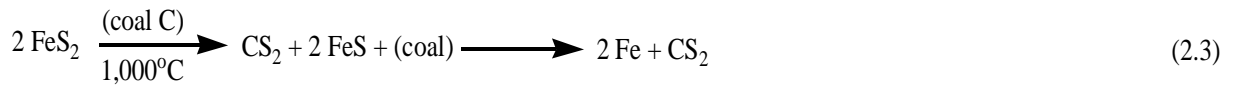
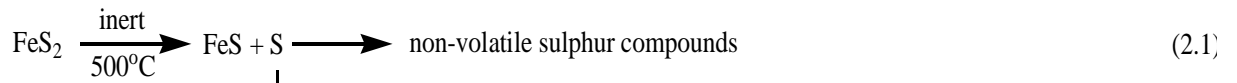
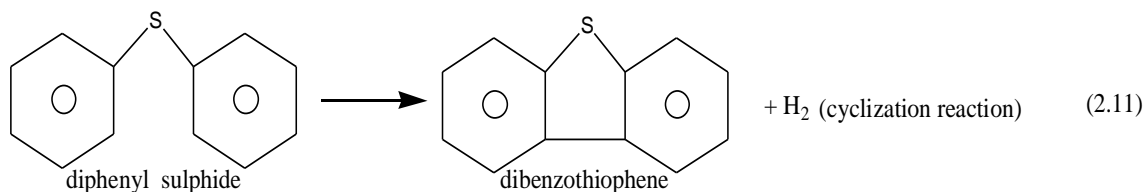
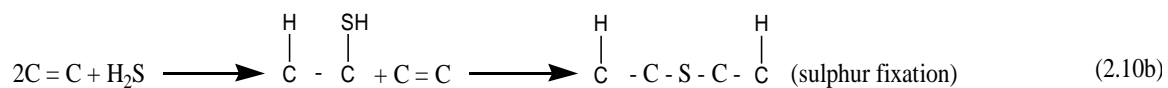
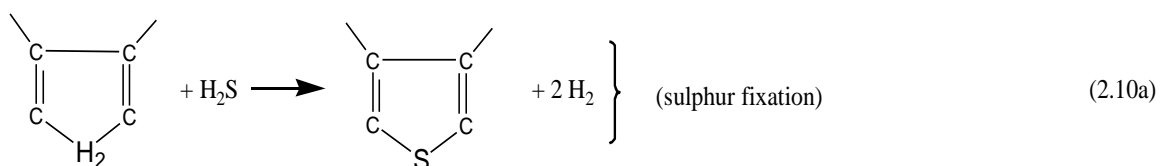
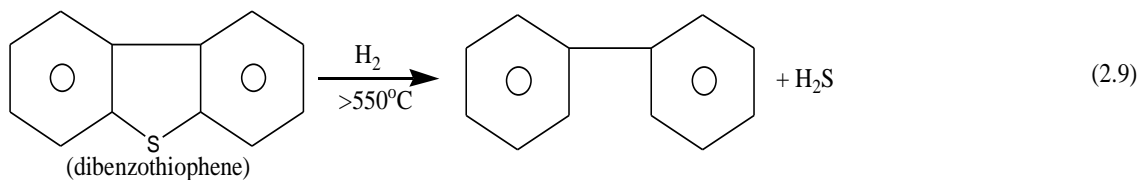
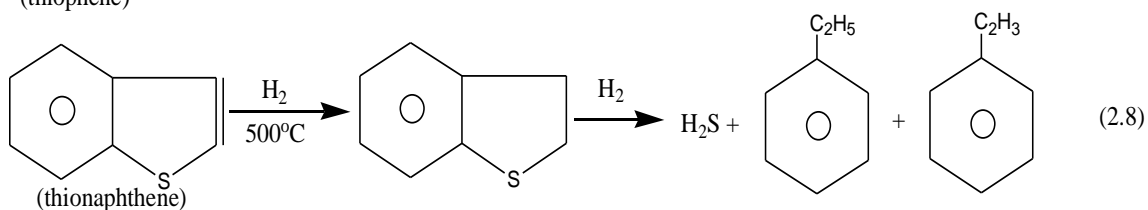
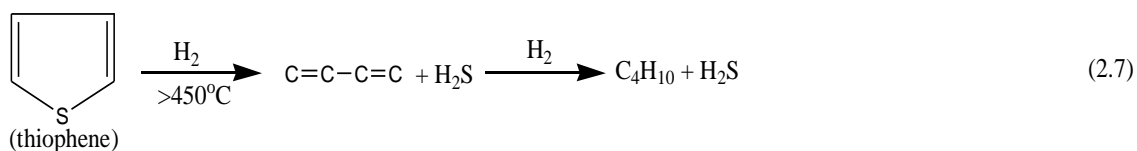


Table 2.3 A summary of possible organic reaction involving sulfur compounds during gasification and pyrolysis process



For example, pyrite in coal is pyrolyzed in inert atmospheres, to sulfide and sulfur at a temperature of 823 K, followed by the reaction between sulfur formed and hydrogen-containing components of coal (coal-H) to form H₂S [11]. The overall reaction can be written as follows [12].



A significant amount of the sulfur is released with these products as H₂S, COS and CS₂. Other forms include substituted and substituted thiophenes, benzothiophenes and dibenzothiophenes. The volatile sulfur species, H₂S is the most abundant of all of the potential species [13]. The percentage of sulfur removed as H₂S decreased as the temperature and duration of carbonization increased [14]. About 33.6% of sulfur was removed from the residue following pyrolysis of Shenhua coal, which 32.1% was H₂S in gas and 1.5% was transferred into tar, 66.4% of the sulfur remained in the residue char [15]. Ibarra et al [16] found that coal samples with higher pyrite contents released very little sulfur as H₂S at >630°C, whereas samples with lower pyrite contents and hence higher organic matter evolved more H₂S. Ibarra [17] investigated the behavior of sulfur structures in low rank coal with high organic and pyritic sulfur contents during low temperature pyrolysis. They found that the evolution of H₂S as a function of temperature passes through two peaks between 500–560 °C and also between 630–700 °C, related to the decomposition of organic and pyritic sulfur, respectively. And the evolution of COS with pyrolysis followed a trend similar to that for H₂S. Moreover, the evolved SO₂ was not only related to the decomposition of iron sulfate from weathering of pyrite, but also with the presence of oxidation reactions during pyrolysis. Miura et al [18] examined the

relationship between the decomposition behavior of each form of sulfur and the formation of sulfur-containing gases. They found that the aliphatic sulfur was decomposed below 500 °C and the aromatic sulfur was decomposed at 400–700 °C accompanying the formation of H₂S and the decomposition of thiophenic sulfur was strongly dependent on coal type. Gryglewicz [19] demonstrated that the effectiveness of high temperature pyrolysis in the removal of sulfur from coal depends on the rank of the latter and the effectiveness of pyrolysis in sulfur removal appears to be related to the proportion of the non-thiophenic sulfur to the total organic sulfur in the coal. Czaplicki [20] found that distribution of total sulfur in coal pyrolysis products is basically affected by coal to air ratio and addition of steam or acceptor to the pyrolysis process. H₂S evolution during coal pyrolysis was found to be a function of temperature up to 850 °C. The low concentration of SO₂ detected for some of the samples is due to decomposition of inorganic sulphates present. Maximum sulfur release was found in the range of 600–850 °C and has a decreasing tendency from 850–1000 °C [21].

The atmosphere of pyrolysis also has an important effect on the evolution of sulfur-containing gases during coal pyrolysis. Carbon monoxide (CO) promotes the formation of carbonyl sulfide (COS); carbon dioxide (CO₂) inhibits the evolution of sulfur-containing gases at temperatures below 600 °C and exhibits effects similar to those of CO above this temperature; methane (CH₄) also inhibits the evolution of sulfur-containing gases at temperatures below 600 °C but promotes the formation of H₂S at temperatures above 800 °C; and hydrogen gas (H₂) improves the formation of hydrogen sulfide (H₂S) and inhibits the formation of other sulfur-containing gases [22]. All of

these gases are present in the SHR in significant amounts. Chen et al [23] investigated the transformation of sulfur in some high sulfur coals from China in a fixed bed reactor under the pressure of 3 MPa at a heating rate of 10 K/min. They also found that sulfur was removed from coal more effectively in hydrolysis than in pyrolysis.

Gasification processes have also received a lot of attention. During CO₂ gasification, there is more COS and less H₂S formation compared with pyrolysis and steam gasification. This is a consequence that CO could react with sulfide to form COS. During steam gasification only H₂S was produced and no COS detected, because H₂ has greater tendency to form H₂S than compared to CO. After steam gasification no sulfur was detected in the gasification residue [15].

A thermal chemical process called Steam Hydrogasification developed by the College of Engineering Center for Environmental Research and Technology (CE-CERT) at the University of California, Riverside (UCR) has been shown to convert carbonaceous feedstock into syngas (H₂ and CO mixture) in a very cost effective manner [24]. Large amount of H₂ and steam exist during the steam hydrogasification process and results in the different behavior of sulfur in the gas phase compared to other thermo-chemical processes.

The major objective of this chapter was to investigate the formation of sulfur species during steam hydrogasification. The effect that the hydrogen partial pressure, temperature and water have on the sulfur composition in the gas phase species was also determined. These results will provide information of developing a sulfur gas clean up

system for protection of the downstream catalysts, and will be the topic of the next chapter.

2.2 Simulation Work

2.2.1 Aspen Simulation

The Aspen model simulates the steam hydrogasification reactor (SHR) using decomposition and gasification units. These units are based on built-in Aspen reactor blocks and calculate the equilibrium composition in the reactor under the given conditions by means of Gibbs free energy minimization. The decomposition block converts the non-conventional feedstock such as biomass or coal into its basic elements on the basis of yield information using the RYIELD block and the gasification block calculates the equilibrium product gas composition using the RGIBBS block. The feedstock is assumed to be mixed with water and the resulting slurry is fed into the SHR block along with the hydrogen at predetermined H_2/C mole ratio and water/feed mass ratios. The carbon conversion information, feed flow rates and compositions, and the reactor operating conditions are supplied by the user [24].

The aim of Aspen simulation is to give some clue for the design of experiment about sulfur distribution in the gas phase during steam hydrogasification process.

2.2.2 Aspen Simulation Results

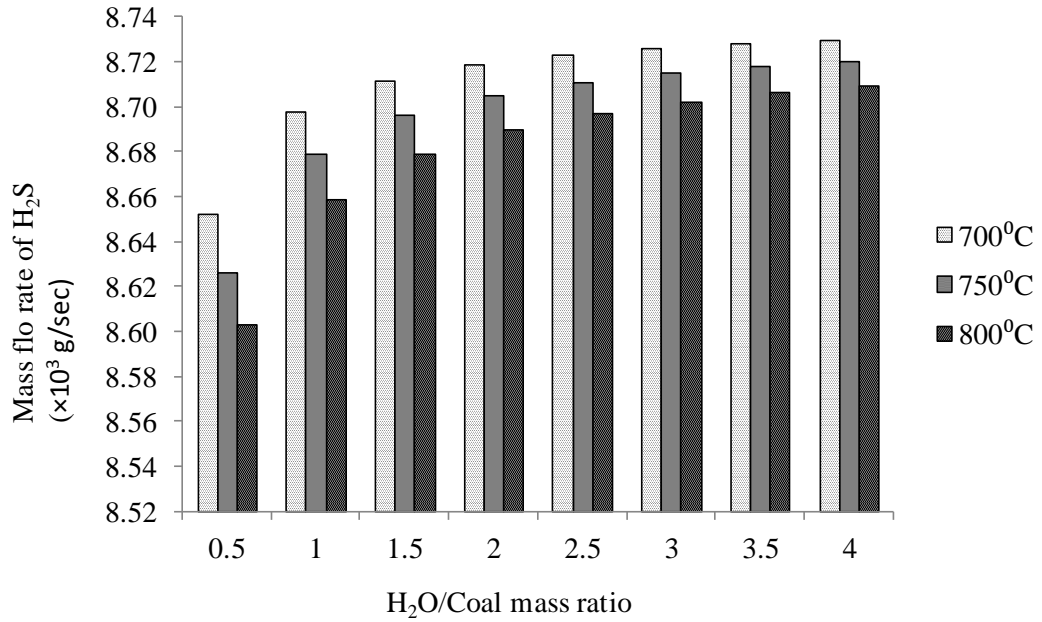


Figure 2.2 H₂O/C mass ratio vs H₂S mass flow rate at different temperature

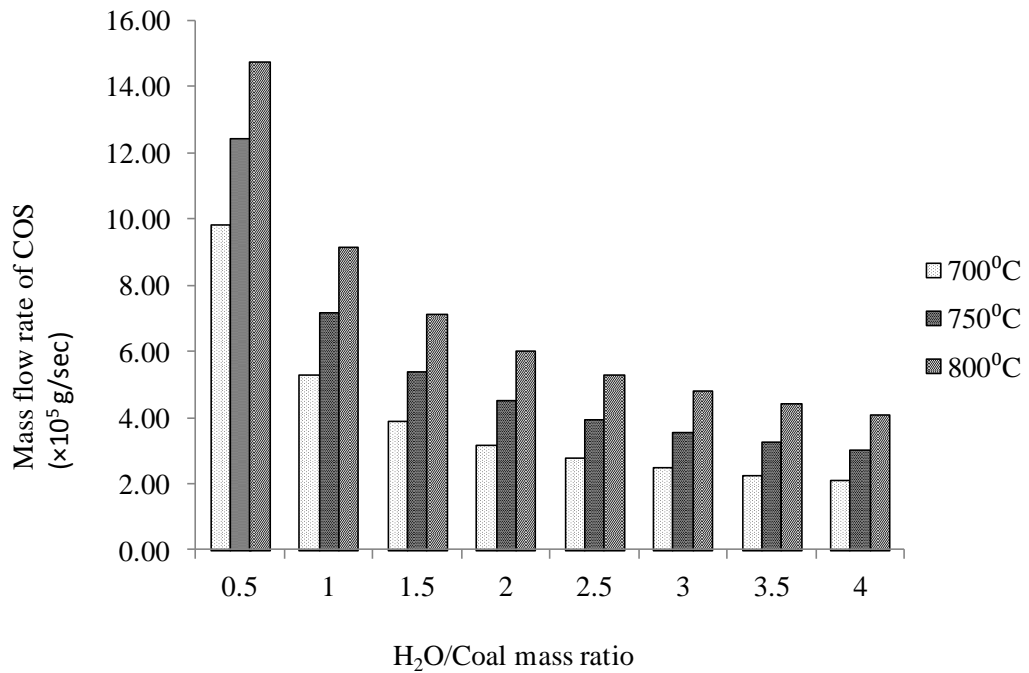


Figure 2.3 H₂O/Coal mass ratio vs COS mass flow rate at different temperature

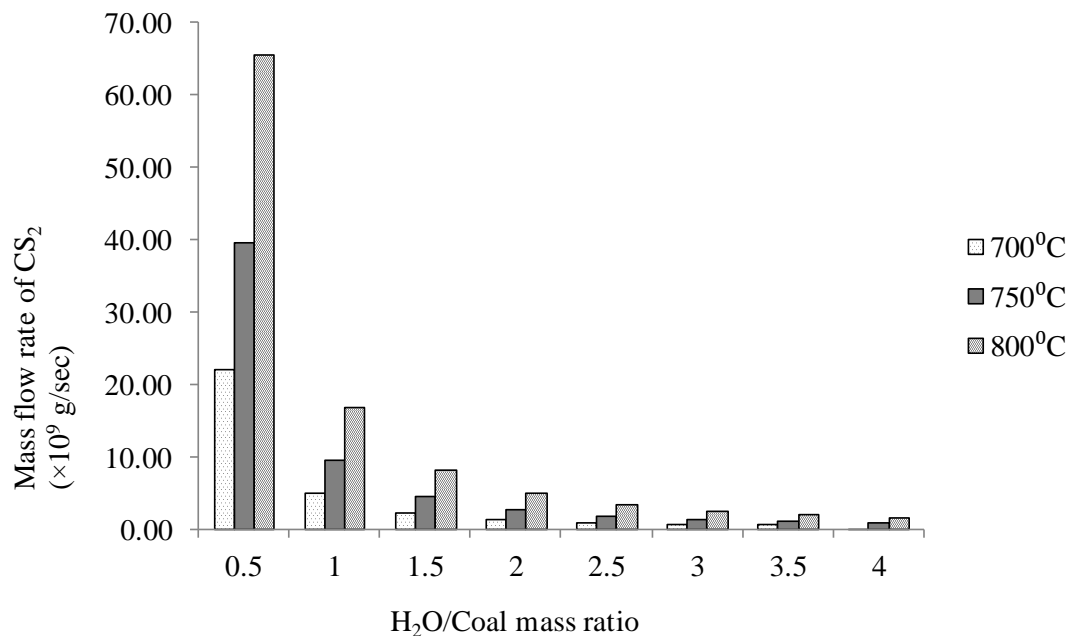


Figure 2.4 H₂O/Coal mass ratio vs CS₂ mass flow rate at different temperature

The results of the simulation showed in Figure 2.2 to Figure 2.4 indicate that the syngas output of the SHR have higher amount of H₂S and lower amount of COS and CS₂. The mass flow rate of H₂S will increase and the mass flow rate of CS₂ and COS will decrease when more water is added into reaction. Based on the simulation result, a series experiment was done to investigate the sulfur distribution in SHR process.

2.3 Experimental Section

2.3.1 Materials

The feed materials are bituminous coal from Illinois region. The feed material is ground to a size of less than 150 μm. The composition of the coal material is given in Table 2.4

Table 2.4 Proximate and ultimate analysis of the coal sample

Ultimate Analysis (Dry Basis)		Proximate Analysis(As received)	
Component	Weight %	Parameter	Weight %
C	67.4	Moisture (M)	3.2
H	5.1	Volatile Carbon	36.2
O	13.3	Fixed Carbon(FC)	50.9
N	1.3	Ash	9.8
S	3.3		

High Heating Value: 12083 Btu/lb

2.3.2 Apparatus

A batch reactor setup with a reactor volume of 260 cc was used for these experiments. The reactor was specifically designed to enable continuous stirring under high pressures. The reactor is made of Inconel® alloy and can be operated at pressures and temperatures as high as 500 psi and 800 °C respectively. A schematic diagram of the reactor system along is shown in Figure 2.5. Figure 2.6 shows a photograph of the reactor setup .The reactor setup is comprised of a heating system, a batch reactor, a water trap, a gas outlet that allows collect product gases to be collected by tedlar gas sampling bag, a data acquisition (DAQ) system monitored using Labview software. The DAQ registers reaction parameters such as temperature, pressure and heater duty into a computer. The reactor and all the pipelines have been treated by Silcolloy 1000 which is a passivation layer inert to sulfur-containing gas provided by Silcotek Company. This was done to minimize the problem of sulfur absorption.

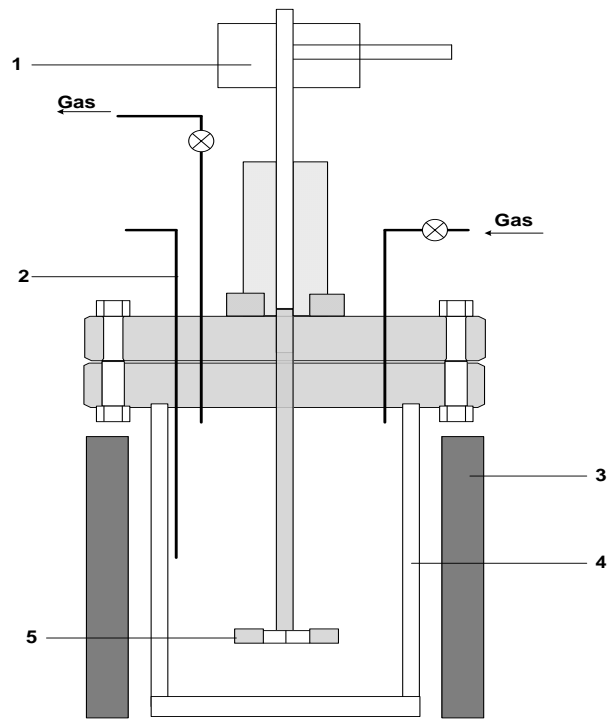


Figure 2.5 Schematic diagram of the stirred batch reactor

(1. Magnetic agitator; 2. Thermal couple; 3. Heater; 4. Reactor; 5. Impeller)



Figure 2.6 Photograph of the stirred batch reactor setup

2.3.3 Experimental Procedure

The feed sample is loaded into the reactor vessel along with the desired water and the reactor is connected to the impeller arrangement and tightened by means of the flange. The reactor is then tested for leaks. The reactor and system is flushed by sulfur gas before the start of each experiment, to confirm that there was no absorption of sulfur gas. Then the reactor is flushed and purged with H_2 three times using a vacuum pump. The reactor is then pressurized with H_2 to a desired pressure. Cooling water is circulated during the test in the space between the reactor and the motor that drives the impeller in order to

avoid damage to the motor due to very high temperatures. The water chiller and the cooling water pump are started well before the start of the test. The chiller is set to a temperature of 4 °C. The reactor is heated by immersing it into a tubular electrical heater at the start of the test. The electrical heater temperature is set at a value of 50 °C higher than the desired reaction temperature. Once the electric heater reached the set temperature, it is raised using a mechanical lift so as to immerse the reactor in the heater and the temperature control is set so that the inside temperature of the reactor is at the desired reaction temperature. The test is carried out until the pressure decreased below 100 psi since carbon conversions did not increase after this point and it is assumed that the reaction is not progressing. The temperature inside the reactor and on the space between the heater and the outside surface of the reactor were monitored by means of thermocouples and the pressure inside the reactor is monitored by means of a pressure transducer. The temperature, pressure and heater duty information were collected every second through the Labview data acquisition system. After the test, the heater is turned off and is lowered and the reactor is allowed to cool down. Once the reactor reached room temperature, the product gas is collected by Tedlar gas bag and the vessel is removed and the unreacted char along with the ash were carefully collected and weighed. The char and ash sample is then vacuum dried at 100 °C for 20 minutes in order to remove any moisture present. The sample is weighed again.

The volatile sulfur-containing product gas from the reactor is analyzed by Gas Chromatography (GC) with flame photometric detector (FPD). GC-FPD has High sensitivity for sulfur and phosphorous, and it is 100,000 times more sensitive to sulfur

compounds than hydrocarbons. The sulfur content in residual char is determined by Huffman Laboratories. All the tests were conducted with half a gram of feed and the amount of liquid water necessary for the desired H₂O/Feed mass ratio.

2.4 Experimental Result and Discussion

2.4.1 Sulfur Formation in the Gas Phase

Any sulfur in the fuel, according to studies by Meng [25], will be converted to primarily hydrogen sulfide(H₂S), with some small amounts of gas phase carbonyl sulfide (COS) and carbon disulphide (CS₂). The formation of sulphuric pollutants during steam hydrogasification can be described as follows [26, 27].



Gas phase reaction:



The experiments of steam hydrogasification and coal yielded no detectable amounts of COS and CS₂. The gas phase reactions (2.13 to 2.16) indicate that both COS and CS₂ are difficult to form due to large amount of H₂ and steam in the reactor. Zhou, et al [27] suggest that the presence of hydrogen gas improves the formation of hydrogen sulfide and inhibits the formation of other sulfur-containing gases. Only H₂S was detected as gaseous S-containing products during coal hydrolysis [15]. Similar phenomena were found during the steam gasification process. There is no COS detected because

above 450°C. Hydrogen could react with COS formed from reaction 2.14[28]. Furthermore, Calkins [11] noted that only above 850°C some CS₂ is formed at the expense of H₂S. Attar [6] concluded that H₂S is the dominant sulfur-containing product for reactions in a H₂ environment.

Since the temperature of the SHR process is process below 850°C with a H₂ and steam-rich environment, the formation of H₂S is favorable and the formation of COS and CS₂ are suppressed. This explains that H₂S is the only gaseous sulfur species detected in the gas phase during the SHR process.

2.4.2 Effect of Temperature

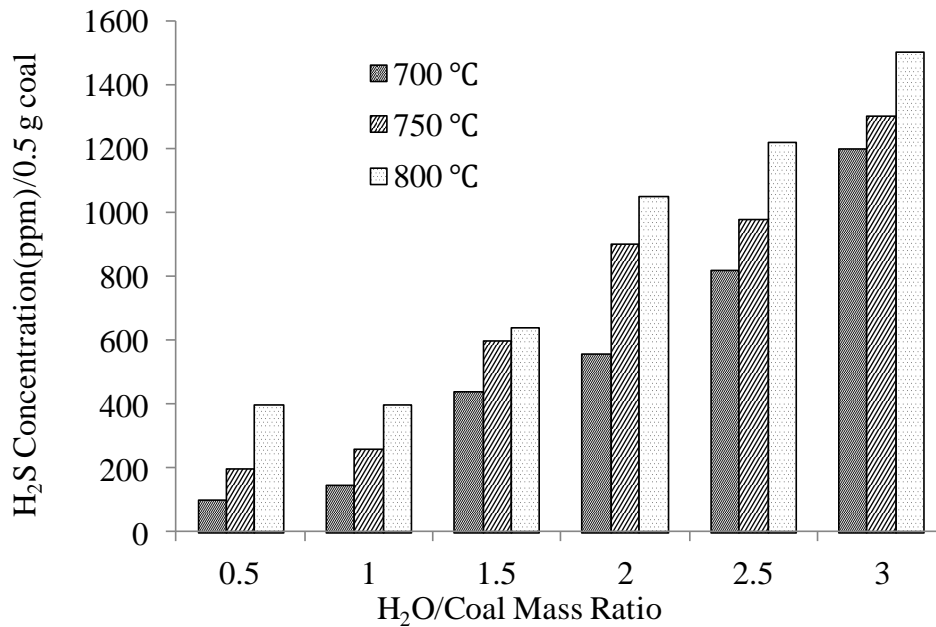


Figure 2.7 The effect of water to coal mass ratio on H₂S concentration at different temperature (Initial H₂ pressure: 50 psi)

It should be expected that release of volatiles of sulfur would increase with the rise in temperature as a result of more sulfur leaving the solid matrix from coal to form

higher amounts of H_2S . This agrees with our results which are presented in Figure 2.7 to Figure 2.10. H_2S concentrations and the mass of sulfur in the gas phase increased with increasing temperature during the steam hydrogasification process. For example, the temperature increase from $700^\circ C$ to $800^\circ C$, at the condition of that the water to coal mass ratio equal to 3 and the initial H_2 pressure is equal to 25 psi, led to an increase of H_2S from 1200ppm to 3000ppm and mass of sulfur released in the gas phase from 2.6mg to 8.0mg respectively, as shown in Figures 2.9 and 2.10.

Similar results were obtained in earlier studies of rapid pyrolysis of coal where the sulfur yield in the gas increased over the range of temperature between $700^\circ C$ - $950^\circ C$ [27]. Another study showed that the sulfur yield in the gas increased linearly with increasing temperature [12] during rapid hydrolysis of coal. This behavior is consistent with the results obtained herein Kuramochi et al [29,30] concluded that lower temperature favors the formation of species such as FeS , ZnS , MnS retained in the solid phase, resulting in lower concentration of H_2S in syngas at lower temperature.

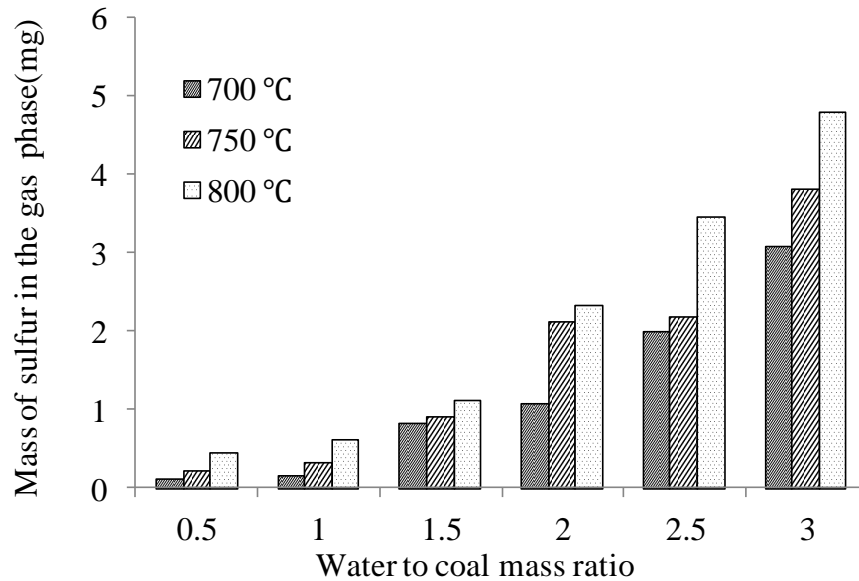


Figure 2.8 The effect of the water to coal mass ratio on the mass of sulfur in the gas phase at different temperature (Initial H₂ pressure: 50psi)

2.4.3 Effect of Steam (Water)

The results presented in Figure 2.7 to Figure 2.10 show that the H₂S concentration and mass of sulfur in the gas phase increased with an increase in the water to coal mass ratio. For example, H₂S increased from 760ppm to 3000ppm and the mass of sulfur in the gas phase increased from 0.6mg to 8.0mg as the water to coal mass ratio increased from 0.5 to 3. These experiments were conducted at 800°C with an initial H₂ pressure of 25 psi. Increasing the water to coal mass ratio from 0.5 to 3 results with the H₂ pressure increased to 50 psi increases the concentration from 400ppm to 1500ppm and mass of sulfur in the gas phase from 0.5mg to 4.8mg. These results can be explained by steam

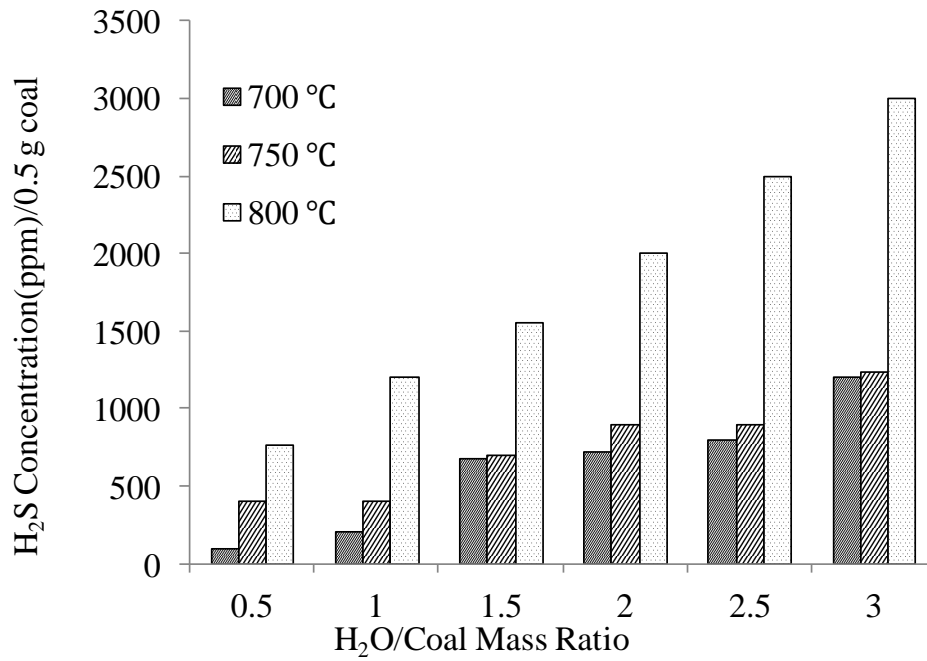


Figure 2.9 The effect of water to coal mass ratio on H₂S concentrations at different temperature (Initial H₂ pressure: 25 psi)

reacting with pyrite to promote the formation of H₂S [31]. Similar results were obtained by Czaplocki [32] , who found that the addition of steam to the pyrolysis process results in the increase of sulfur in gas phase.

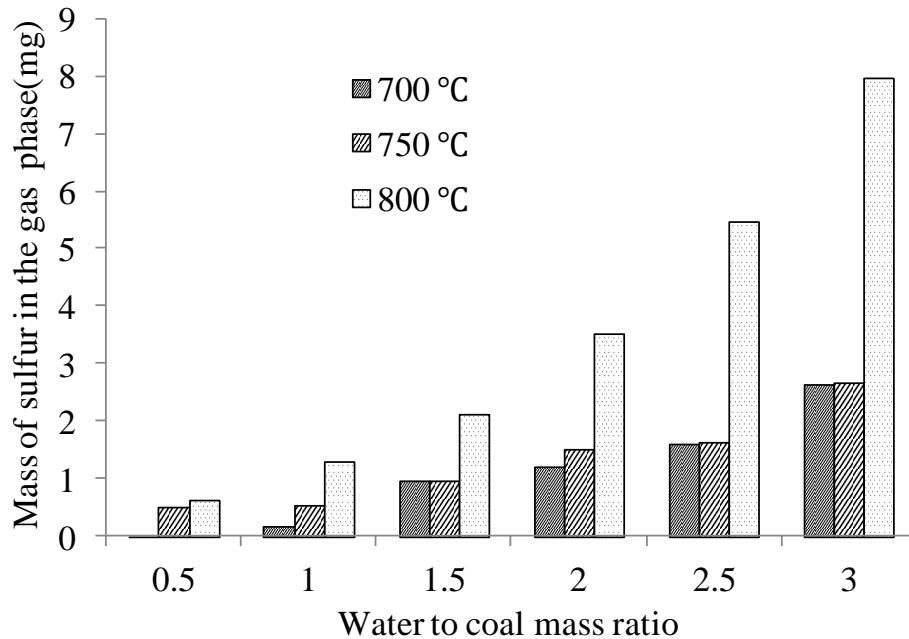


Figure 2.10 The effect of water to coal mass ratio on the mass of sulfur in the gas phase at different temperature (Initial H₂ pressure: 25 psi)

2.4.4 Effect of H₂ Partial Pressure

The concentration of H₂S and the mass of sulfur in the gas phase decreased when the initial H₂ partial pressure increased from 25 psi to 50 psi at 800°C. These results are shown in Figure 2.11. The sulfur in the gas phase increased by 67% when the hydrogen pressure decreased from 50 psi to 25 psi when the water to coal mass ratio is equal to 3.

Chen, et al [23] claimed that hydrolysis provided a more effective method of desulfurization than pyrolysis because H₂ help H₂S formation during coal hydrolysis. However, such results conflicted with Cleyle's theory [32] which states that in a hydrogen-rich environment H₂S will be trapped by active carbon generated by devolatilization of the coal matrix as it is diffused away from the FeS-coal interface

through the pores of the matrix. This will lead to pyritic sulfur converted into organic sulfur. When the H_2 partial pressure increased, more H_2S is released by the decomposition of pyrite combined with the organic matrix. This is a possible explanation that sulfur in the gas phase reduced while increasing H_2 partial pressure.

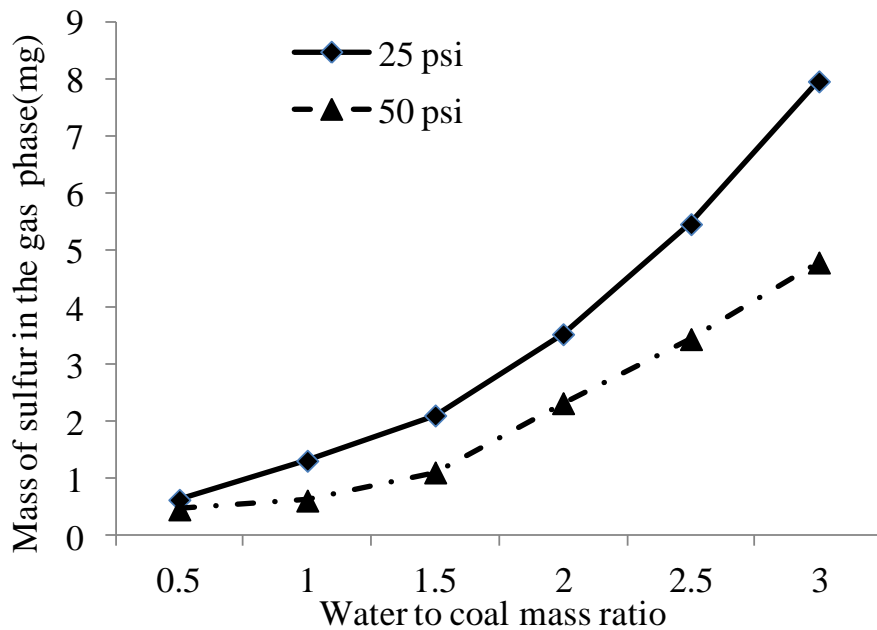


Figure 2.11 H_2 partial pressure effect on the mass of sulfur in the gas phase at $800^\circ C$

2.5 Conclusion

The important results of our study are summarized below. These results were obtained during the steam hydrogasification process with coal as the feedstock.

- 1) H_2S is the only sulfur containing species detected in the gas phase in the SHR with typical process conditions. No COS and CS_2 was detected. The result is promising. Not only because COS and CS_2 are difficult to remove compared with H_2S , but also carbon is wasted if it was converted into COS and CS_2 .

Elimination of both COS and CS₂ will increase the potential of the carbon conversion to synthesis gas.

- 2) The formation of H₂S increased with increasing temperature in the reactor, which can be explained as more sulfur leaving the solid matrix of coal with higher temperatures. At the same time, H₂S increased when the water to coal mass ratio increased. The possible reason for this is that steam reacts with pyrite promoting the formation of H₂S.
- 3) H₂S was reduced with increasing H₂ partial pressure. It is speculated that H₂S produced by decomposition of pyrite will be captured by the organic matrix at the higher H₂ partial pressure.

It has been shown by this work that under typical SHR process conditions, the formation of gaseous sulfur species is affected by the major process variables. Our results generally agree with the previous findings of other studies using similar gasification conditions. The SHR operates at lower temperatures and high water concentrations. These experimental results provide important information for designing a sulfur cleanup process to remove the sulfur-containing process for protection downstream catalysts used for steam reforming and Fisher-Tropsch reaction processes.

References

1. A. Demirbas, Sustainable cofiring of biomass with coal, *Energy Conversion Management*, 2003, 44(9), 1465–1479.
2. D.A Tillrman., Biomass cofiring: the technology, the experience, the combustion consequences, *Biomass and Bioenergy*, 2000, 19(6), 365-384.
3. A. Ros, Dried sludges and sludge-based chars for H₂S removal at low temperature: influence of sewage sludge characteristics, *Environmental Science & Technology*, 2006, 40(1), 302-309.
4. J.G. Speight., *The chemistry technology of coal*, New York, 1983.
5. A. Czaplicki., W. Smolka, Sulfur distribution within coal pyrolysis products. *Fuel Processing Technology*, 1998, 55(1), 1-11.
6. A. Attar, Chemistry, thermodynamics and kinetics of reactions of sulphur in coal-gas reactions: a review, *Fuel*, 1978, 57, 201-212.
7. M.R Khan., Prediction of sulfur distribution in products during low temperature coal pyrolysis and gasification, *Fuel*, 1989, 68(11), 1439-1449.
8. G. Gryglewicz., Sulfur transformations during pyrolysis of a high sulfur polish coking coal. *Fuel*, 1995, 74(3), 356-361.
9. F. Liu, et al., Sulfur transformation during pyrolysis of Zunyi coal by atmosphere pressure-temperature programmed reduction-mass spectrum, *Journal of Fuel Chemistry and Technology*, 2008. 36(1), 6-9.
10. K. Sugawara., et al., Effect of heating rate and temperature on pyrolysis desulfurization of a bituminous coal. *Fuel Processing Technology*, 1994, 37(1), 73-85.
11. W.H. Calkins, Investigation of organic sulfur-containing structures in coal by flash pyrolysis experiments, *Energy & Fuel*, 1987, 1, 59-64.
12. W.C. Xu, M. Kumagai, Sulfur transformation during rapid hydrolysis of coal under high pressure by using a continuous free fall pyrolyzer, *Fuel*, 2003, 82, 245-254.
13. F. Garcis-Labiano, W. Hampartsoumian, A. Williams, Determination of sulfur release and its kinetics in rapid pyrolysis of coal, *Fuel*, 1995, 74, 1072-1079.

14. K. Ceylan, A. Olcay, Low temperature carbonization of tuncbilek lignite. Effectiveness of carbonization for desulfurization, *Fuel Processing Technology*, 1989. 21(1), 39-48.
15. X. Chu, et al., Sulfur transfers from pyrolysis and gasification of direct liquefaction residue of Shenhua coal. *Fuel*, 2008. 97(2), 211-215.
16. J. Ibarra, et al., Evidence of reciprocal organic matter-pyrite interactions affecting sulfur removal during coal pyrolysis. *Fuel*, 73(7), 1046-1050.
17. J.V. Ibarra, A.J. Bonet., R. Moliner, Release of volatile sulfur compounds during low temperature pyrolysis of coal. *Fuel*, 73(6), 933-939.
18. K. Miura., et al., Analysis of Formation Rates of Sulfur-Containing Gases during the Pyrolysis of Various Coals. *Energy Fuels*, 2001, 15(3), 629-636.
19. G. Gryglewicz, Effectiveness of high temperature pyrolysis in sulfur removal from coal. *Fuel Processing Technology*, 1996, 46(3), 217-226.
20. A. Czaplicki, W Smolka., Sulfur distribution within coal pyrolysis products. *Fuel Processing Technology*, 1998, 55(1), 1-11.
21. B.P. Baruah, P. Khare, Pyrolysis of high sulfur Indian coals, *Energy Fuels*, 2007, 21(6), 3346-3352
22. Q. Zhou, et al., The atmosphere of pyrolysis also have important effect on evolution of sulfur-containing gases during coal pyrolysis. *Energy Fuels*, 2005, 19(3), 892-897.
23. H. Chen, et al., Transformation of sulfur during pyrolysis and hydrolysis of coal. *Fuel*, 1998, 77(6), 487-493.
24. C.S. Park, S.P. Singh, J.M. Norbeck, Steam hydrogasification of carbonaceous matter to liquid fuels, *Proceedings of the 24th Annual International Pittsburgh Coal Conference*, Johannesburg, South Africa, 2007.
25. X.M. Meng, W.D. A.H. Jong, M. Verkooijen, Thermodynamic analysis and kinetics model of H₂S sorption using different sorbents, *Environmental Progress & Sustainable Energy*, 2009, 28, 360-371.
26. R. Zevenhoven, P. Kilpinen, Control of pollutants in flue gases and fuel gases, third edition, Espoo, Finland, 2004.

27. Q. Zhou, H. Hu, Q. Liu, S. Zhu, Effect of atmospheres on evolution of sulfur containing gases during coal pyrolysis. *Div., Fuel Chem.*, 2004, 49, 927-928.
28. H. Chen, B. Li, B. Zhang, Effects of mineral matter on products and sulfur distributions in hydrolysis, *Fuel*, 1999, 78, 713-719.
29. M. Dial , I. Gulyurtlu. H₂S and HCl formation during RDF and coal co-gasification: a comparison between the predictions and experimental results. INETI- DEECA, Est. Paço do Lumiar, 22, 1649-038 Lisboa, Portugal.
30. H. Kuramochi, D. Nakajima, S. Goto, K. Sugita, W. Wu. HCl emission during copyrolysis of demolition wood with a small amount of PVC film and the effect of wood constituents on HCl emission reduction, *Fuel*, 2008, 87, 3155-3157.
31. D. Shao, E.J. Hutchinson, J. Heidbrink, W. Pan, C. Chou, Behavior of sulfur during coal pyrolysis, *Journal of analytical and applied pyrolysis*, 1994, 20, 91-100.
32. P. J. Cleyle, W.F. Caley, I. Stewart, S.G. Whiteway, Decomposition of pyrite and trapping of sulphur in a coal matrix during pyrolysis of coal, *fuel*, 1984,63, 1579-1582.

Chapter 3 Hydrogen Sulfide Removal from Syngas Produced by Steam Hydrogasification Reaction

3.1 Desulfurization Technologies

We can see from Chapter 2 that hydrogen-sulfide (H_2S) is the predominate sulfur containing contaminant evolved as a result of coal that are subjected through the SHR. The removal, or better the reduction of H_2S concentration, is necessary prior to the product gases entering the steam-methane reforming (SMR) followed by the Fischer-Tropsch (FT) units; otherwise, high concentrations of H_2S will cause poisoning and deactivation of the catalysts that are present in these reactor units [1-3].

There have been several methods investigated by other researchers for the removal of H_2S , which includes cold gas cleanup involving scrubbing H_2S with an amine-based system and warm gas cleanup involving H_2S removal using sorbent technology [4].

3.1.1 Selexol Scrubbing

Amines can solve H_2S and CO_2 in two different ways depending on the properties of the solvent and the ability of building a chemical bond with the amines [5]. Conventional commercial scrubbing H_2S system is Selexol process showed in Figure 3.1 [5]. The Selexol process is a well-proven, stable acid gas removal based on the use of dimethyl ether of polyethylene glycol as a physical solvent [6]. The system is based on physical solubility, and the driving force is the high solubility of H_2 and CO_2 and other acid gases compared to other light gases. No chemical reactions (i.e. acid-base reactions) occur [6]. Higher partial pressures lead to higher solubility of all components, but the attractiveness of the Selexol system is the solvent tends to dissolve H_2S better than

gaseous compounds of comparable volatility. Therefore, the Selexol process is ideally suited for the selective removal of H₂S [6, 7].

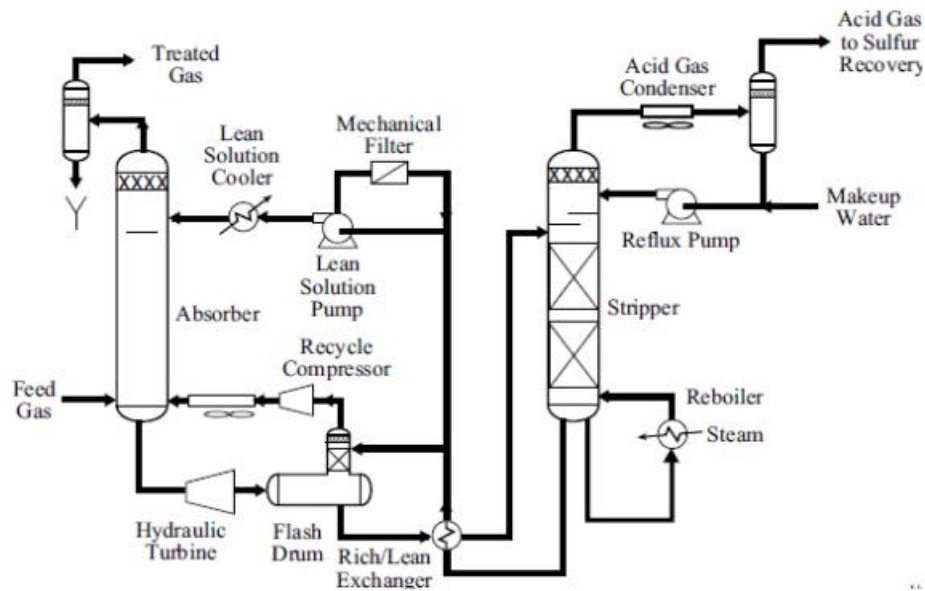


Figure 3.1 Conventional Selexol process for removal H₂S from syngas

Selexol process is more effective for high H₂S partial pressure applications [8]. And the process is subject to process equipment corrosion, foaming, amine-solution degradation, and amine solution evaporation [9].

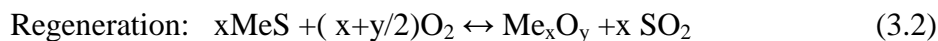
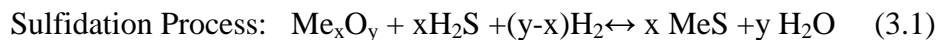
3.1.2 Warm Gas Cleanup

H₂S removal by using sorbent has been received a lot of attention. The extensive research and development work on the sorbent technology mainly metal oxide in this decade has culminated in a number of sorbent compositions that are near commercialization. The choice of metal oxide for the sorbent depends on the temperature of interest and the degree of sulfur removal requirement.

Cold gas clean-up would not be an effective means to remove the H₂S from the CE-CERT process because of the consideration of the overall energy utilized. Energy will be wasted if the steam produced in the SHR is cooled to room temperature to remove the sulfur and then heated to steam again for the SMR. In order to avoid the high capital cost, energy losses & complexity of totally cooling the hot raw syngas leaving the steam hydrogasifier, a warm gas clean-up which reduce cost of fuel gas cooling and associated heat exchangers has been proposed with the aid of a metal oxide [10-11].

3.2 Metal Oxide Sorbents Screening

Metal oxides (MeO), are known to have sulfur capturing capability. The following reaction is observed when H₂S is reacted with a metal oxide [12];



The choice of a primary metal oxide depends on the temperature of interest and the degree of sulfur removal required. The optimum desulfurization temperature appears to be in the range of 350- 550°C, where technical viability and process efficiency result in a lower overall process cost. In addition, because of the more favorable thermodynamic equilibrium in this moderate temperature range, a large number of metal oxides are potentially capable of reducing the H₂S concentration below 20ppmv, increasing the likelihood of developing suitable sorbents [13].

Based on the equilibrium constants and Gibbs free energies, it was pointed out that eleven metal oxides of iron (Fe), zinc (Zn), molybdenum (Mo), manganese

(Mn), vanadium (V), calcium (Ca), strontium (Sr), barium (Ba), cobalt (Co), copper (Cu) and tungsten (W) had thermodynamic feasibility for desulfurization for low-Btu gases in a temperature range 300°C-1400 °C, defined as a H₂S removal efficiency of more than 95% and the existence of thermal stable components [14]. It was concluded, as the thermodynamic analysis shown in Figure 3.2 and Figure 3.3 [12], that the following list of metals are potentially useful for developing metal oxide-based sorbents for fuel gas desulfurization in the moderate temperature range: Fe, Cu, Mn, Zn, Mo, Co, and W.

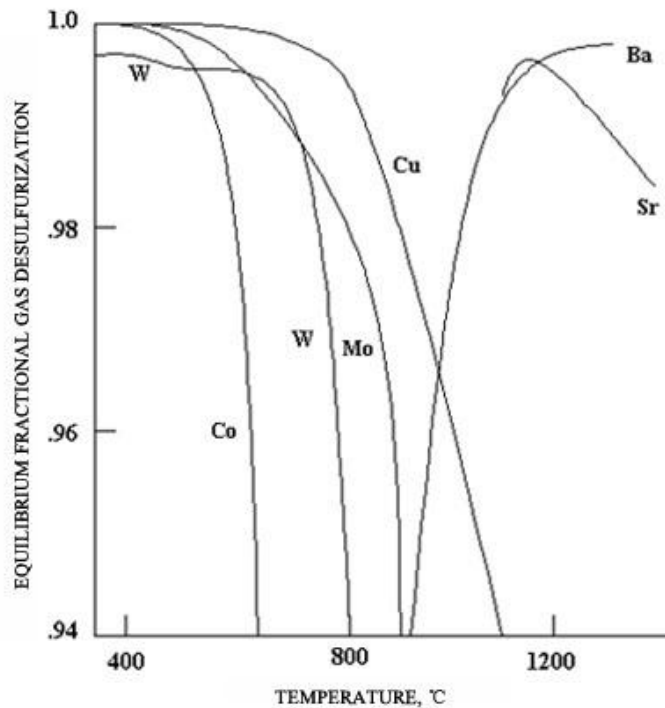


Figure 3.2 Temperature vs desulfurization efficiency of potential metal solid candidates

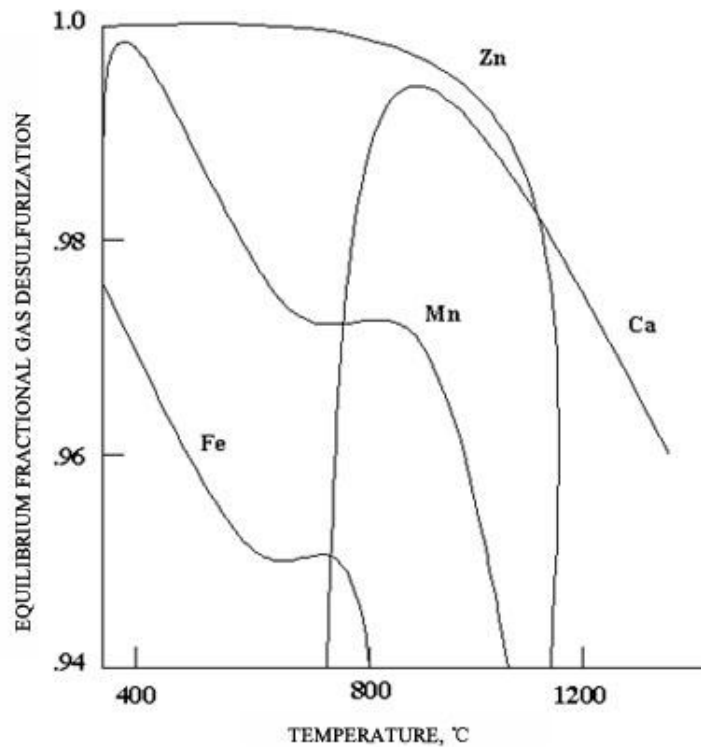
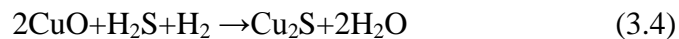


Figure 3.3 Temperature vs desulfurization efficiency of potential metal solid candidates

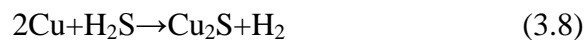
Both molybdenum and tungsten oxides have good desulfurization potential; however, they are temperature-limited because of possible carbide formation. Cobalt exhibits similar behavior to that of copper in its tendency to reduce to the metallic form in fuel gas atmospheres. Desulfurization with cobalt oxide is more temperature-limited compared to copper oxide, and becomes less efficient with increasing temperature. In addition, cobalt sulfide requires significantly higher temperatures for regeneration than copper sulfide. For these reasons, sorbents based on oxides of Cu, Fe, Mn, and Zn has been studied in most cases [14].

3.2.1 Copper Oxide Based Sorbents

Copper-based sorbents have been widely investigated because of the favorable equilibrium between copper oxides and H₂S. The reactions between H₂S and copper oxides at low temperatures were described by Patrick et al. , see reaction 3.4 and reaction 3.5 [15].



The theoretical capacities are 0.21 g H₂S/ g Sorbent for CuO, and 0.24 g H₂S/g of Sorbent for Cu₂O, which are only one third of CaO sulfur capacity or 50% of ZnO sulfur capacity. Moreover, copper oxides are not the stable in highly reducing gases, such as reformates, they are prone to be reduced to metallic copper even at low temperatures via reactions 3.6 and 3.7. They both are rapid reactions and metallic copper becomes the active sorbent for H₂S removal according to reaction 3.8 [16]:



3.2.2 Iron Oxides Based Sorbents

Iron oxides, one of the best metal oxides candidates for H₂S removal, have been studied extensively in 1970s and 1980s. Iron oxide desulfurization potential is somewhat lower compared to the other materials. The sulfidation reactions of iron oxides are following [17]:





According to reactions 3.9 and 3.10, FeO has a capacity of 0.47 g H₂S/g sorbent; Fe₃O₄, 0.44, compared with 0.42 of ZnO. Focht et al. indicated that iron oxides such as Fe₃O₄ were more reactive than Fe metal. And Fe₃O₄ showed less-desulfurization capability at a temperature of lower than 600 °C compared to FeO and Fe₂O₃. Therefore, iron oxides are suitable for fuel gases with low reducibility [18].

However, iron oxide based sorbents have some drawbacks for practical use. The sulfur capacity drops severely in the presence of water [19]. In highly reducing gases containing large fraction of H₂ or CO, such as reformates and coal gas, iron oxides become unstable and reduced to metallic iron. For example, at 700 °C, Fe₃O₄ was found to be reduced to FeO in presence of coal gas, which showed detrimental effects on sulfidation reactivity [18]. At temperatures above 500 °C, the excess iron reduction and iron carbide formation lead to severe sorbent decrepitation [18, 20, 21]. Another drawback is high temperatures, eg. 850°C, are required to regenerate FeS without sulfate formation [22].

3.2.3 Manganese Oxide Based Sorbents

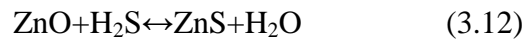
Among all manganese oxides, MnO is the stable oxide phase in reducing atmospheres, including the highly reducing environments and slightly reducing environments. MnO maintains this feature even at high temperatures (T>750 °C)[23,14, 24]. Therefore, manganese based sorbents are exceptionally suitable for desulfurization of highly reducing gases at high temperatures. The sulfidation of MnO is described by reaction 3.11.



Advantage of manganese based sorbent is that the manganese sulfide can be regenerated at temperatures above 750 °C to void sulfate formation, which means both sulfidation and regeneration of MnO sorbents can be conducted at the same temperature [25]. However, manganese oxide based desulfurization sorbents including MnO are not thermodynamically favorable for H₂S removal. Another possible disadvantage of MnO is the effect of CO₂ at temperature below 400°C due to MnCO₃ formation [14].

3.2.4 Zinc Oxide Based Sorbents

The thermodynamics of H₂S removal using ZnO is superior to most other metal oxides and H₂S concentration in the product gas can be reduced to less than 10ppmv. The main reaction of ZnO sulfidation is described as follows [14];



The Gibbs free energy of the above reaction is $\Delta G = -91607.18 + 15.16 T$ (J/mol). Therefore, conversion of ZnO to ZnS can easily take place at low temperature including room temperature [26, 27]. It was reported that ZnO is thermodynamically favorable at low temperatures ($T < 500$ °C). At high temperatures ($T > 550$ °C), zinc loss in reducing fuel gases becomes significant [14].

Pure ZnO has a high stoichiometric capacity of 0.42 g H₂S/g ZnO. In practice the saturation sulfur capacity of commercial ZnO extrudates can reach >60% of the stoichiometric value depending on the process temperature, flow conditions and sorbent properties [28].

3.2.5 Reaction Schemes

In the reaction between H_2S and ZnO , H_2S molecules must first diffuse to the surface of the ZnO . There, H_2S reacts with ZnO to form ZnS , and the H_2O formed must diffuse away. Finally, the sulfide ion must diffuse into the lattice and the oxide ions diffuse to the surface. Under normal conditions, the equilibrium is strongly in favor of sulfide formation; but at lower temperatures, overall rate of reaction is controlled by pore and lattice diffusion [29]. As a result, only part of the ZnO is converted to ZnS . Sasaoka described the reaction scheme between ZnO and H_2S in $\text{H}_2\text{S-H}_2\text{-CO}_2\text{-H}_2\text{O-CO}_2\text{-N}_2$, as shown in Figure 3.4 [30].

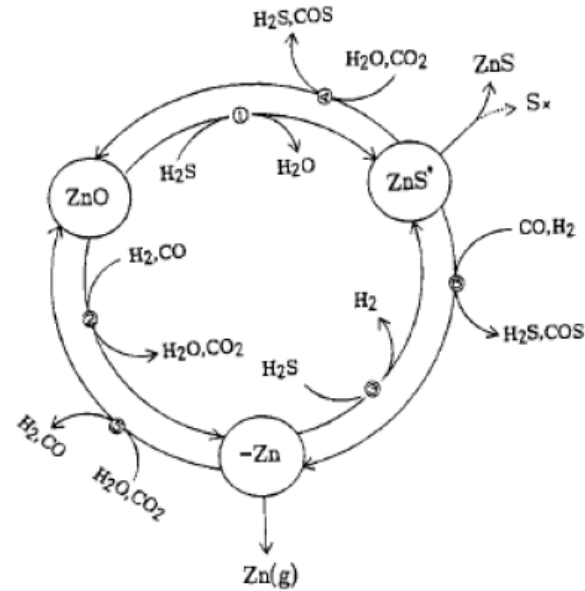


Figure 3.4 Scheme of reaction between ZnO and H_2S in $\text{H}_2\text{S-H}_2\text{-CO}_2\text{-H}_2\text{O-CO}_2\text{-N}_2$

The reaction between ZnO and H_2S can be accelerated by H_2 and CO . At 400°C , H_2 can not reduce ZnO in the presence of H_2O , as a result, the reaction between ZnO and H_2S is inhibited. At 500°C , H_2 can reduce ZnO to $-\text{Zn}$ and hence accelerate reaction

between ZnO and H₂S. CO₂ can inhibit the reduction of ZnO similar to H₂O, but it plays a complicated role in the reaction because its ability to prevent the reduction of ZnO is smaller than that of H₂O [30].

Steam present in gaseous fuel reversibly reformates, inhibited the H₂S sorption by shifting reaction 3.12 from right side to the left side. Sasaoka et al. [30] showed that sulfur capture capacity of ZnO sorbent decreased in the presence of 20 vol% steam as compared with the case of little or no steam in the feed stream and Kwon et al. [31] demonstrated that sulfur absorption by metal oxide sorbent was reduced when steam content of feed gas increased from 0 to 20 vol%. Novochinskii et al. [32] also reported that steam in sulfidation of ZnO inhibits H₂S removal capability. Kim et al found that 45% of steam in steam hydrogasifier product gas result in decreasing the sulfur capture capacity of the sorbent, which may require more frequent replacement of sorbent to avoid the deactivation of catalyst for downstream reaction.

Hydrogen can reduce ZnO to element zinc during its sulfidation at 500°C, as a result, the reaction between ZnO and H₂S is inhibited [30]. The high concentrations (>10%) of H₂ increase the reaction rate between ZnO and H₂S that was explained by the change of basicity of ZnO surface in presence of H₂ [33]. CO inhibited the sulfidation reaction and formed COS when H₂ was absent from the system; ZnO was reduced by H₂ and/or CO at 500 °C and followed by zinc vaporization when H₂O and/or CO₂ were absent [34]. In a later study, Sasaoka et.al found ZnS catalyzed the conversion of COS to H₂S in the presence of H₂O and H₂ [30].

In this chapter, one group of mixture gas which simulated the composition of syngas produced by SHR was chosen as the inlet gas stream to investigate the H₂S breakthrough time and ZnO sulfur capture capacity at the temperature of 623K. Space velocity was varied as the major parameter of the evaluation. Moreover, the effect of mixture gas containing H₂, CO, CO₂ and CH₄ on sorbent sulfur capture capacity and H₂S breakthrough time was investigated. In addition, each component of mixture gas effect on sulfidation process has been studied.

3.3 Experimental Setup and Analytic Methods

3.3.1 Sorbent

In this study, the zinc oxide sorbent was provided by Sud-Chemie Incorporated. The physical properties of the sorbent were listed in Table 3.1. The sorbent was crushed and was sieved to obtain the appropriate particle size. 150-250 μm was chosen which has proved to be small enough to eliminate the effect of inter-particle mass transfer limitation in the previous study in the literature [35].

Table 3.1 Properties of zinc oxide sorbent

ZnO content (%)	Max 90%
Surface area(m ² /g)	50
Bulk density(g/cm ³)	1.35
Pellet size(mm)	4.76

3.3.2 Desulfurization Setup

The experiments apparatus consisted of four parts: a gas mixing chamber, a reactor, water trap and gas chromatography. A schematic diagram of the apparatus is shown in Figure 3.5. If not addressed, all the gases were purchased from Praxair, Inc. In the gas supply system, H₂S-N₂ cylinders with 10.0 vol. % supplied H₂S for the reaction. H₂, CO, CO₂, CH₄, N₂ of high purity gas was employed and balance the gas concentration needed.

The reactor was made from a quartz tube (16mm o.d., 12mm i.d., 450 mm long) and was enclosed by an electric heater. The sorbents were loaded at the center of the reactor. Two flat layers of glass wool of 9 μm were put on the top and the bottom of the packed sorbents. These layers distributed the gas flow and kept the sorbent particles from moving. Glass beads, which were inert to H₂S, supported the bed and these two wool layers (showed in Figure 3.6).

In the setup, the temperature was measured by K-type thermocouple, which was inserted to the mid-depth of the sorbent bed in the reactor. And the temperature was controlled by a PID-type temperature controller. After the gas stream left the reactor, it passed through a moisture trap made of calcium chloride (CaCl₂).

H₂S concentration of the feed gas and exit gas from the reactor were measured by a gas chromatography (Hewlett-Packard 5890 series II) equipped with a flame photometric detector (FPD). Every sample of 250 μL was collected right after the reactor every ten minutes, and injected manually to the FPD.

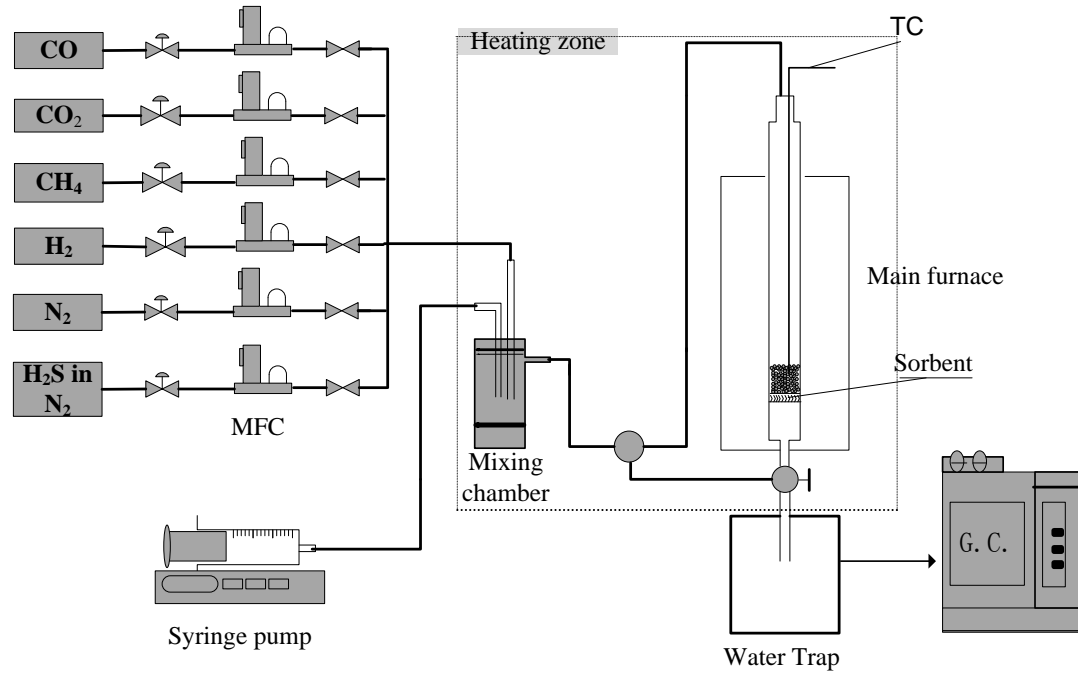


Figure 3.5 Schematic diagram of the experimental apparatus

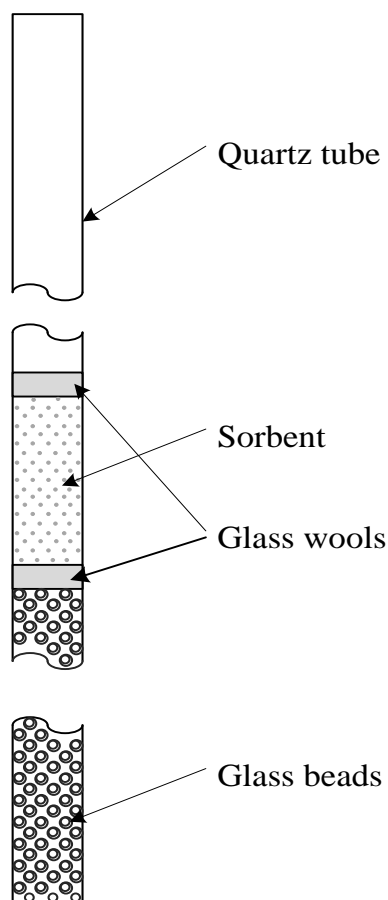


Figure 3.6 Reactor used in desulfurization system

3.3.3 Flow Rate Control

Mass flow controllers (Unit Instrument series) were used to control the mass flow rate during experiment. All of them were calibrated carefully before experiments. The calibrations of pure gas were done by using Drycal gas flow meter, which has been calibrated by the manufacture. However, the calibration of $\text{H}_2\text{S-N}_2$ mixture cannot be calibrated by Drycal gas flow meter because of H_2S erosion. Therefore, the flow rate of $\text{H}_2\text{S-N}_2$ mixture was calibrated specially with a soap bubble meter.

3.3.4 Steam Generation

In this study, the water was introduced to reaction system in form of steam. As showed in Figure 3.5. The mixture gas passed through the mixing chamber and carried saturated steam into reactor. In order to keep the water in vapor phase, the tubing from the mixing chamber was wrapped in heating tapes. The amount of water in gas was controlled by changing the scale of pump, which can control the mass input of water into system.

3.3.5 GC Calibration

The GC-FPD detector was calibrated for the H₂S response. The square root of FPD response area should be linear to the H₂S concentration. The calibration curve is showed in Figure 3.7.

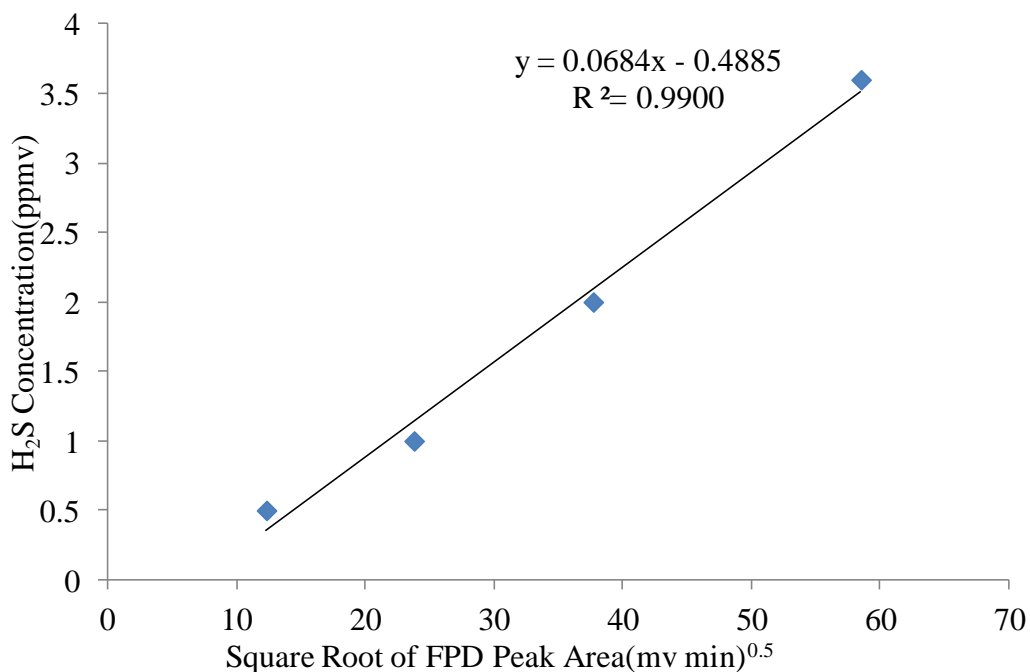


Figure 3.7 Relationship between the square root of FPD peak area and H₂S concentration

3.3.6 Experimental Procedure

During a typical experiment, 0.35-1.40g ZnO sorbent was loaded into the fixed-bed quartz reactor, depending on the space velocity tested. Reactant gases were added to quartz reactor using compressed gas cylinder, which was controlled by mass flow controller (MFC). Calibration of the MFC's was performed for all gases used. A mini-pump was used to inject liquid H₂O into the mixing chamber. Once the gas stream, containing varying amounts of H₂, CO, CO₂, CH₄, H₂O and N₂, was adjusted to desired concentrations, an H₂S adsorption experiment was started. The exit gas was cooled in a water trap and was then passed through a moisture-trap containing desiccators located before the gas chromatography. Every experiment will be conducted three times to obtain consistent and repeatable results. The sulfur capture capacity (grams of sulfur per 100 g of sorbent, g sulfur/100 g sorbent) of the sorbent was calculated using the following formula [32]:

$$S_{cap} = \frac{FR \times \int_0^{BT} (C_{in} - C_{out}) dt \times 32 \times (1 \times 10^{-4})}{V_{mol} \times m_{sorbent}} \quad (3.13)$$

Where S_{cap} is the sulfur capture capacity (in units of g S/100 g of sorbent), BT is the breakthrough time (in hours) measured when the outlet H₂S concentration reaches the breakthrough threshold, and t denotes the time that elapsed after the start-up of sorbent sulfidation. FR is gas flow rate (in units of L/min), V_{mol} is the molar volume (24.45 L/mol, under standard conditions). C_{in} and C_{out} are the inlet and outlet H₂S concentration (in units of ppmv), 32 refers to the molecular weight of sulfur, $m_{sorbent}$ is the sorbent weight (in grams), and 1×10^{-4} is the normalizing coefficient, adjusting the

units. All the experiments were performed at the atmospheric pressure, and the outlet H₂S concentration of 2 ppmv was used as the threshold to determine the breakthrough of sorbent sulfidation.

3.4 Result and Discussion

3.4.1 Effect of Space Velocity on H₂S Adsorption

Figure 3.8 and 3.9 shows the effect of space velocity upon H₂S breakthrough time and sulfur capture capacity respectively for the inlet gas with 1000 ppmv H₂S concentration. 1000 ppmv was selected to simulate the sulfur content of product gas from SHR. Figure 3.8 shows that the breakthrough time for 2 ppmv H₂S at the reactor outlet decreased from 27.8 h to 4.8 h as the space velocity increased from 6000h⁻¹ to 24000 h⁻¹. Theoretical maximum sulfur capacity is 35.4 (g of sulfur)/ (100g of sorbent). By calculating sulfur capacity according to equation 2, the sulfur capacity was 21.7 (g of sulfur)/ (100g of sorbent) at the space velocity of 6000h⁻¹, which accounting for 61% of the theoretical maximum. This may be a good evidence of good solid-gas contact in the packed-bed reactor at 6000 h⁻¹. Moreover, the sulfur capacity decreased by 21.8% when the sulfur capacity increased from 6000h⁻¹ to 12,000h⁻¹.

Decrease the space velocity increased the sulfur capacity by increasing the time that the gas remains on the ZnO surface. The reaction between ZnO and H₂S is a non catalytic gas-solid reaction. According to Szekely's theory [12], chemical-reaction played a significant role, which can be regarded as rate-limited step. Because ZnO with 150-250µm has been chosen to eliminate the effect of inter-particle mass transfer limitation. Therefore, the higher space velocity resulted in shorter contact time between H₂S gas and

ZnO particles, leading to high outlet H₂S concentration and shorter breakthrough time. In equation 2, it was found that sulfur capacity decreased with increasing C_{out} and decreasing BT.

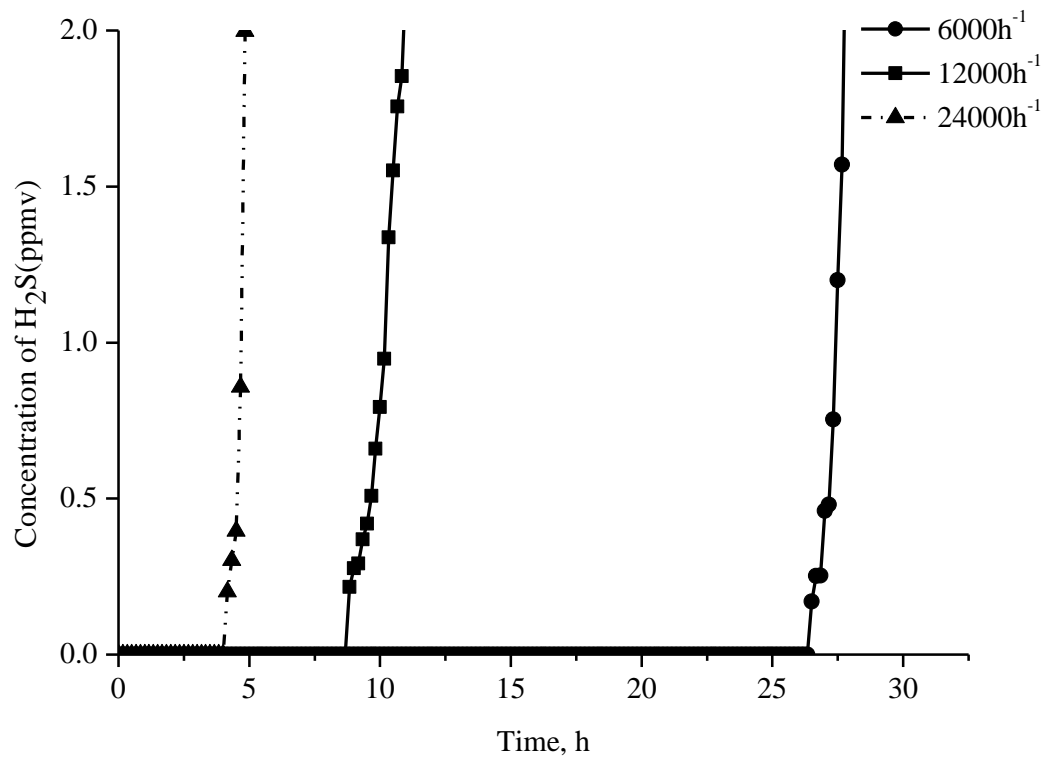


Figure 3.8 Effect of space velocity on H₂S breakthrough time

(Inlet H₂S concentration: 1000 ppmv; Syngas: 45% steam, 32.8% CH₄, 12.2% H₂, 8.3% CO, 1.7% CO₂)

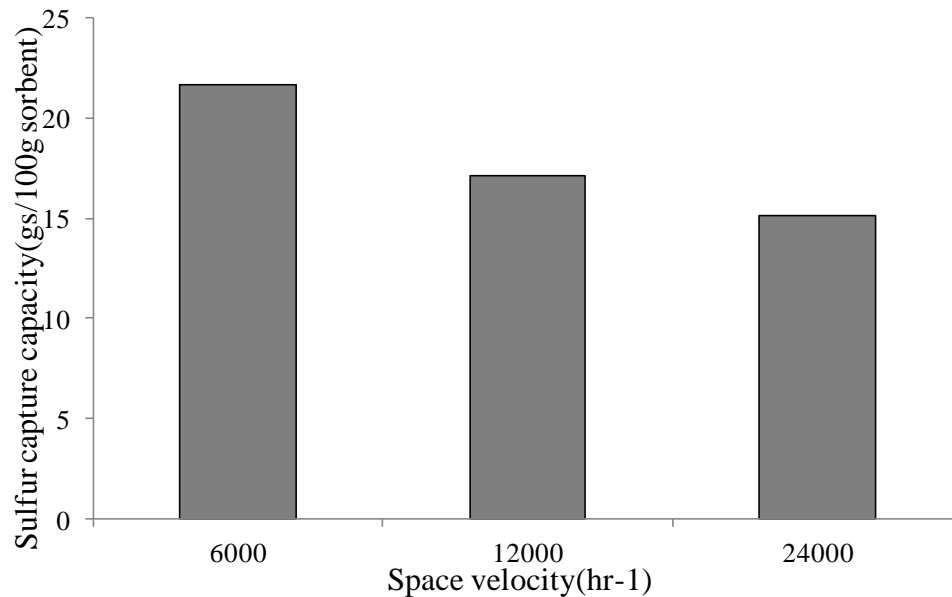


Figure 3.9 Effect of space velocity on H₂S on sulfur capture capacity for H₂S

breakthrough time

(Inlet H₂S concentration: 1000 ppmv; Syngas: 45% steam, 32.8% CH₄, 12.2% H₂, 8.3% CO, 1.7% CO₂)

3.4.2 Effect of Gas Composition on H₂S Adsorption

It was concluded that in the previous study increasing the steam content of the inlet gas resulted in decreasing the sulfur capacity of the sorbent [35]. Besides steam, in the syngas produced by steam hydrogasification process, there are some amounts of H₂, CH₄, CO and CO₂. In order to investigate those gas composition effects on adsorption process, the breakthrough time curve was compared between mixture gas (including H₂, CH₄, CO and CO₂) and nitrogen as the challenge gas at the different space velocity.

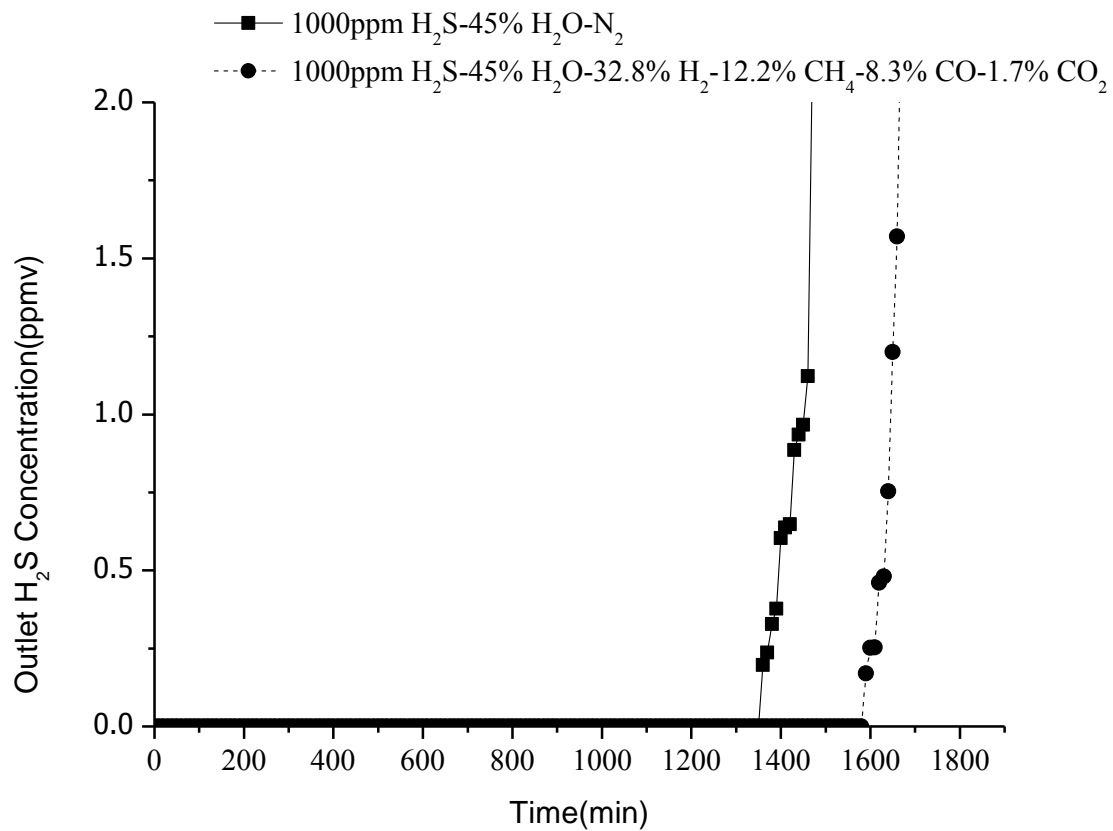


Figure 3.10 Effect of gas composition on H₂S breakthrough time with 6000 h⁻¹ space velocity

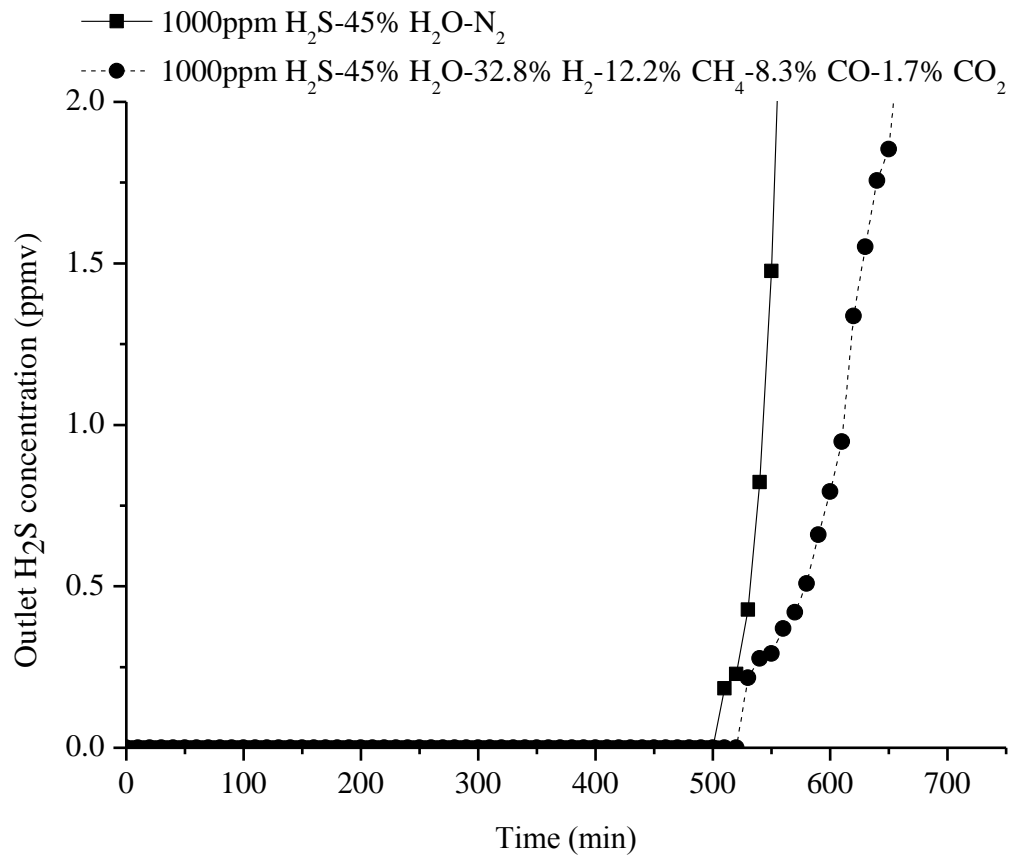


Figure 3.11 Effect of gas composition on H₂S breakthrough time with 12000 h⁻¹ space velocity

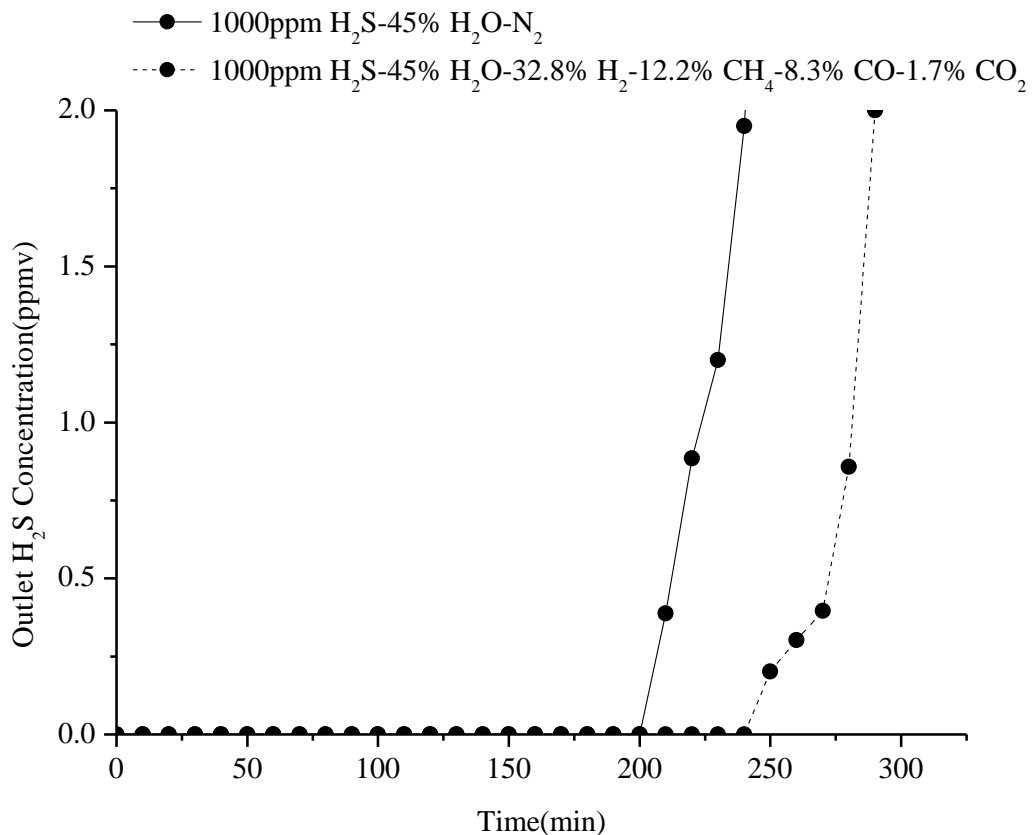


Figure 3.12 Effect of gas composition on H₂S breakthrough time with 24000 h⁻¹ space velocity

As seen in the Figure 3.10, adding CH₄, CO, CO₂ and H₂ to the inlet gas increased breakthrough time from 1470 minutes to 1660 minutes at 6000 h⁻¹ space velocity. Similar trends have been observed at 12000 h⁻¹ space velocity and 24000 h⁻¹ space velocity (Figure 3.11 and Figure 3.12). The breakthrough time increased from 560 minutes to 660 minutes and from 240 minutes to 290 minutes respectively. In the H₂S-H₂-CH₄-CO-CO₂-H₂O system, it is thought that mixture gas containing H₂, CH₄, CO and CO₂ played an important role in the reaction between H₂S and ZnO. In order to investigate the role of

every single gas in the reaction, the 12000h^{-1} was selected to investigate the effect of single gas component on breakthrough time in wet gas.

3.4.2.1 Addition of H_2 in Inlet Gas Stream

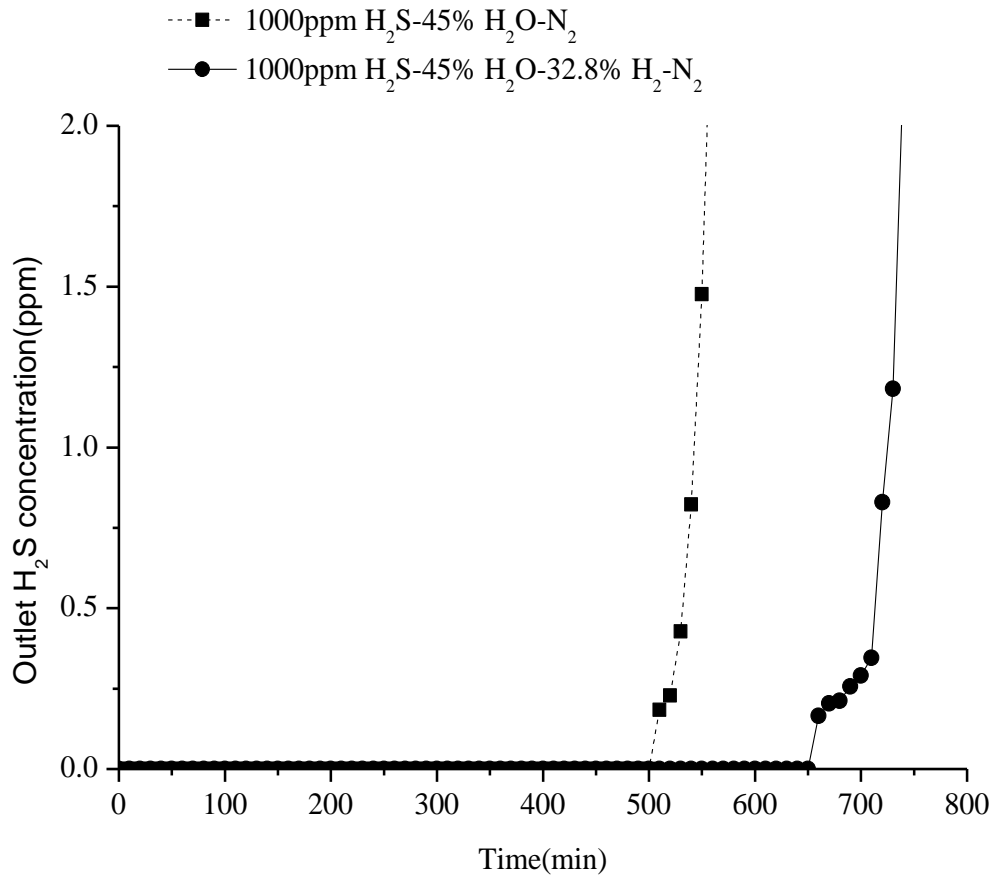


Figure 3.13 Effect of H_2 on H_2S breakthrough time

Hydrogen is the main component in syngas from steam hydrogasification reaction. According to Sasaoka, H_2 may accelerate the reaction between ZnO and H_2S at high temperature and inhibit the reaction at low temperature [30]. The primary desulfurization reaction between ZnO and H_2S is showed in following reaction 3.14. Sasaoka observed

that H₂ can reduce ZnO to Zn according to reaction 3.15 and hence accelerates the reaction between ZnO and H₂S [30].



Addition of H₂ to the inlet gas stream had a positive effect on breakthrough time (Figure 3.13). Adding H₂ to the inlet gas increased breakthrough time from 550 minutes to 730 minutes. The reason of this effect may be related to the performance of the ZnO surface in the H₂.

According to the previous study [37], the first step in the desulfurization should be the adsorption of H₂S on the ZnO surface. So the reaction activity between ZnO and H₂S is related to the basicity of the ZnO. ZnO is a typical n-type semiconductor [38, 36], gas adsorption behavior at the ZnO surface is closely related to ZnO's electron concentration on the surface and its semiconductor's performance. The higher of surface electron concentration is, the stronger of basicity of the ZnO surface is. H₂S is an acid gas. Therefore, an increasing in electron concentration would enhance the basicity of the ZnO surface, which would be beneficial to the adsorption of H₂S, and consequently increase the activity of desulfurization.

H₂ is not involved into desulfurization reaction, but H₂, giving the electron, is easily to be absorbed on the ZnO surface and basicity on the surface of ZnO was then enhanced. Therefore, ZnO surface electron concentration increased and the desulfurization activity were enhanced [36].

3.4.2.2 Addition of CH₄ to the Inlet Gas Stream

As seen with the breakthrough curve in Figure 3.14, adding of CH₄ to the inlet gas stream was found to have the most positive effect of all inlet gases on breakthrough time. Breakthrough time curve shifted to the right side and increased from 550 minutes to 780 minutes.

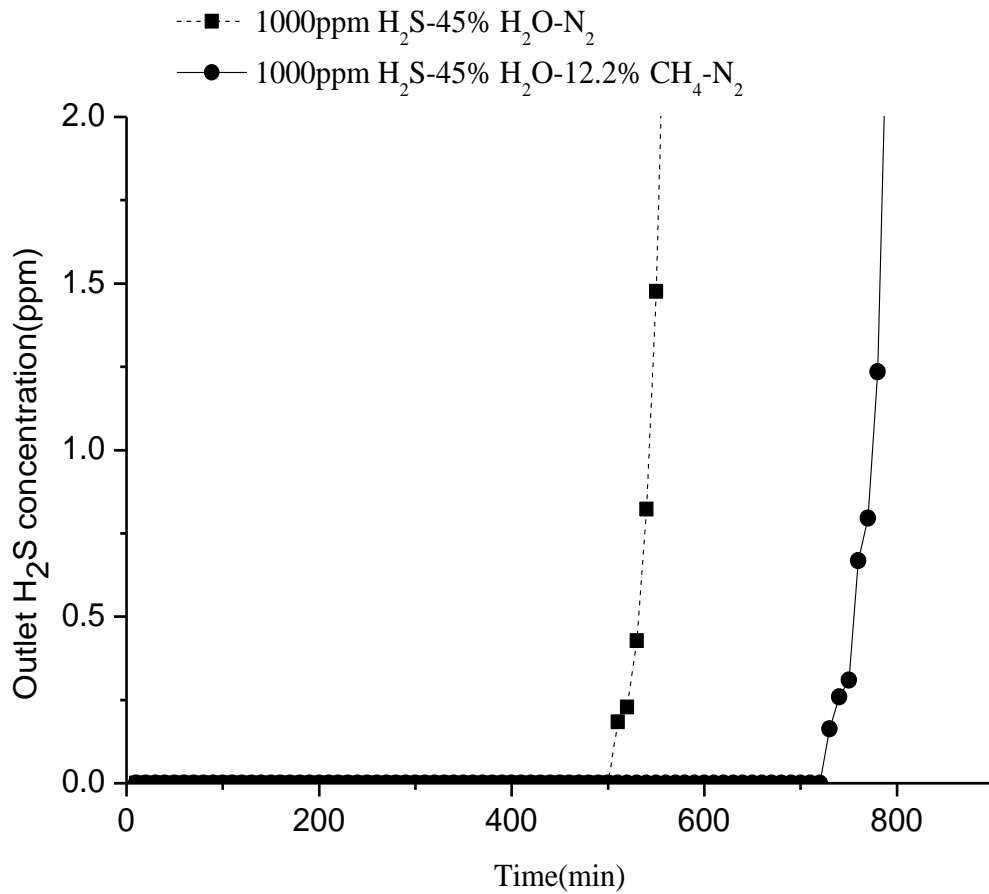


Figure 3.14 Effect of CH₄ on H₂S breakthrough time

The reason that adding CH₄ into inlet gas stream prolonged the breakthrough time may be the same reason as H₂. CH₄ will donate the electron when they are absorbed on

the ZnO surface, and the basicity at the surface of zinc oxide sorbent was then changed. And such change is beneficial for the absorption of H₂S. As a result, adding of CH₄ into inlet gas stream has a positive effect on H₂S absorption by zinc oxide.

3.4.2.3 Addition of CO to the Inlet Gas Stream

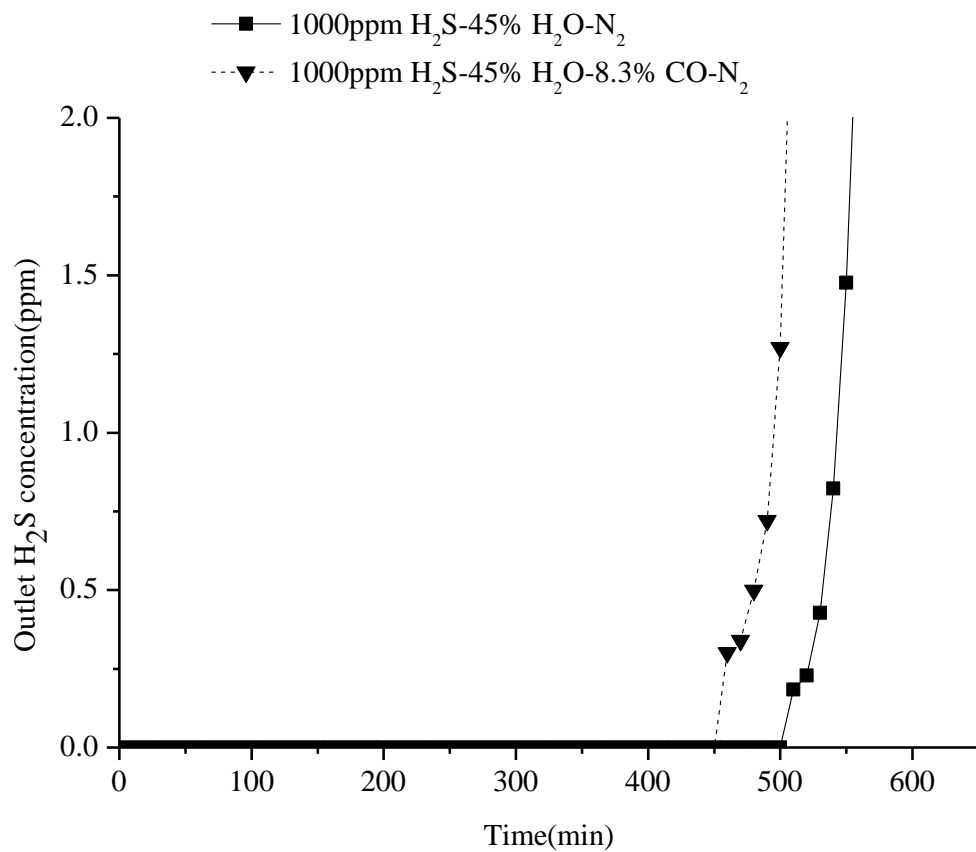


Figure 3.15 Effect of CO on H₂S breakthrough time

It was reported that CO has strong influences on the reaction between ZnO and H₂S. CO chemisorptions on the ZnO may be a cause of the inhibition the reaction between ZnO and H₂S [30].



This adsorbed CO blocks the surface of ZnO and thus inhibits the reaction. It was also thought that a portion of the CO adsorbed on ZnS stabilized the surface. Therefore, CO inhibited the reaction between ZnO and H₂S at 500°C.

Figure 3.15 showed that the presence of CO shifted breakthrough time to the left side and decreased the sulfur capture capacity of ZnO. After the H₂S absorption tests where feed gas contained CO, a grey color of ZnO was observed, indicating carbon formation occurred on the ZnO surface via Boudouard reaction [39]:



It was believed that carbon deposit caused by adding CO into inlet gas poisoned the sorbent, which also hinder the adsorption of H₂S at the surface of ZnO.

3.4.2.4 Addition of CO₂ to the Inlet Gas Stream

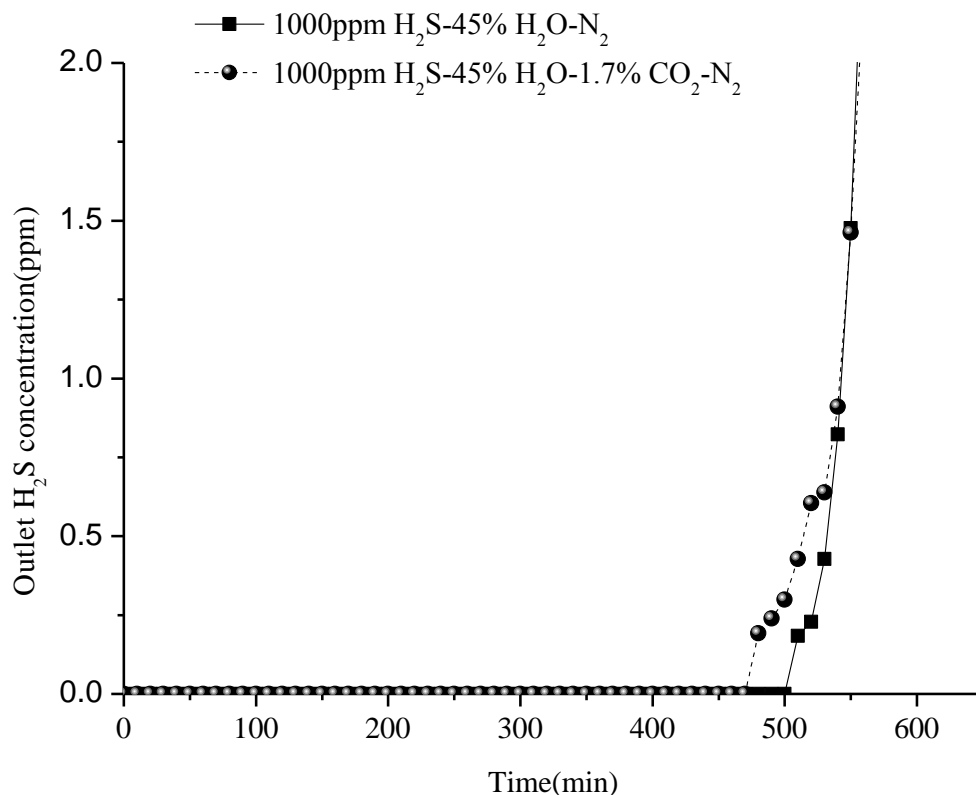


Figure 3.16 Effect of CO₂ on H₂S breakthrough time

When dry CO₂ was present in the reaction system, dry CO₂ can hardly affect the desulfurization process. However, the case was different when CO₂ coexisted with water vapor in reaction system. It was reported that dry CO₂ did not affect the desulfurization behavior may be that absorption of CO₂ on ZnO surface was very difficult in the experimental temperature range. While when CO₂ coexisted with H₂O in the system, the competitive adsorption between two acid gases, CO₂ and H₂S, resulted in a decrease of reaction rate [36].

As can be seen in the Figure 3.16, the addition of CO₂ can hardly effect the breakthrough time. But the shape of breakthrough time curve did shift to the left side. It was reported that adding up to 10% CO₂ has a negative effect on the H₂S breakthrough time [36], but the CO₂ content is low in the coal steam hydrogasification reaction. Thus, adding low concentration of CO₂ into the inlet gas can barely effect the breakthrough time.

3.5 Conclusion

The ability of zinc oxide sorbent to remove H₂S was examined as a function of space velocity and gas composition. The conclusions are summarized as follows.

- 1) H₂S breakthrough time and sulfur capture capacity increase as the space velocity decreased, which caused by longer contact time between gas H₂S and solid ZnO.
- 2) The adding of mixture gas containing CO, CO₂, CH₄ and H₂ into inlet gas has the positive effect on breakthrough time.
- 3) Addition of H₂ or CH₄ to the inlet gas stream increased the breakthrough time and may be related to the adsorption of H₂ and CH₄ on the ZnO surface, which could enhance the basicity of the ZnO surface.
- 4) Addition of CO to the inlet gas stream decreased the breakthrough time. Because carbon deposit on the surface of ZnO hindered the reaction between ZnO and H₂S and adversely affect breakthrough capacity. And, low concentration of CO₂ in the inlet gas stream almost have no influence on the H₂S breakthrough time.

As a conclusion, the syngas from steam hydrogasification reaction containing CO, CO₂, H₂ and CH₄ are beneficial to the reaction between ZnO and H₂S. It compensates, to some extent, the negative effect brought by high steam content in syngas from steam hydrogasification reaction.

References

1. J. Konningen, K. Sjostrom, Sulfur-deactivated steam reforming of gasified biomass. *Ind. Eng. Chem. Res.*, 1998, 37(2), 341-346.
2. C. H. Bartholmew, P. K. Agrawal, and J.R. Katzer, Sulfur Poisoning of Metals, *Advances in Catalysis*, 1982, 31, 135-242.
3. D.J. Duvenhage, N.J. Coville, Deactivation of a precipitated iron Fischer–Tropsch catalyst— A pilot plant study, *Applied Catalysis A: General*, 2006, 298, 211-216.
4. K. Ibsen. Equipment design and cost estimation for small modular biomass systems, synthesis gas cleanup, and oxygen separation equipment.
5. D. J. Kubek, E. Polla, and F. P. Wilcher. Purification and recovery options for gasification. In *Proceedings of Gasification Technology in Practice*, Assolombarda, Milan, Italy, February, 1997.
6. J.W. Sweny, "Gas Treating with a Physical Solvent", AICHE Meeting, Anaheim, CA, Mar. 1984.
7. *Gas Processes 2004, Hydrocarbon Processing*, Gulf Publishing Company, 2004.
8. D. I. Kubek, E. Polla and F. P. Wilcher. Purification and recovery options for gasification. UOP.25 East Algonquin Road. Des Plaines, Illinois 60017-5017 U.S.A.
9. A. Kohl, R. Neilsen, 1997, *Gas Purification*. Gulf Publishing Company.
10. J.S.Rao, J.Neelima, G.Srikanth. A techno-economic comparison of IGCC power plants with cold gas cleanup and hot gas cleanup units using Indian coals. *Proceedings of IJPGC 003, 2003 international joint power generation conference*. Atlanta, Georgia, USA
11. R. Gupta, B. Turk, M. Lesemann. RTI/Eastman warm syngas clean-up technology: intergration with carbon capture. Presentation, 2009 gasification technologies conference.
12. T.A. Aysel, P.H. Douglas, *Desulfurization of hot coal gas*. 1998, Berlin, New York, Springer.
13. R. B. Slimane, J. Abbasian, Regenerable mixed metal oxide sorbents for coal gas desulfurization at moderate temperatures, *Advances in Environmental Research*, 2000, 4 (2), 147-162.

14. P.R. Westmoreland, D. P. Harrison, Evaluation of candidate solids for high-temperature desulfurization of low-btu gases. *Environ. Sci. Technol.*, 1976, 10(7), 659-661.
15. V. Patrick, G.R. Gavalas, M. Flytzani-Stephanopoulos, K. Jothimurugesan, High-Temperature sulfidation-regeneration of CuO-Al₂O₃ sorbents, *Industrial & Engineering Chemistry Research*, 1989, 28, 931-940.
16. S.S. Kamhankar, M. Bagajewicz, G.R. Gavalas, P.K. Sharma, M. Flytzani-Stephanopoulos, Mixed-Oxide sorbents for high-temperature removal of hydrogen sulfide, *Industrial and Engineering Chemistry Process Design and Development*, 1986, 25, 429-437.
17. E. Sasaoka, T. Ichio, S. Kasaoka, High-Temperature H₂S removal from coal-derived gas by iron ore, *Energy & Fuels*, 1992, 4, 603-608.
18. G.D. Focht, P.V. Ranad, D.P. Harrison, High-Temperature desulfurization using zinc ferrite: reduction and sulfidation kinetics. *Chemical Engineering Science*, 1988, 43, 3005-3013.
19. E.C. Oldaker, A.M. Poston, Jr, W.L. Farrior. Laboratory evaluation of properties of fly ash-iron oxide absorbents for H₂S removal from hot low-btu gas. U.S. Energy and Development Administration, Morgantown Energy Research Center.
20. R. E. Ayala, D. W. Marsh, Characterization and long-range reactivity of zinc ferrite in high-temperature desulfurization processes, *Industrial & Engineering Chemistry Research*, 1991, 30, 55-60.
21. R. Gupta, S.K. Gangwal, S.C. Jain, Development of zinc ferrite sorbents for desulfurization of hot coal gas in a fluid-bed reactor, *Energy & Fuels*, 1992, 6, 21-27.
22. M.C. Woods, S.K. Gangwal, D. P. Harrison, K. Jothimurugesan, Kinetics of the reactions of a zinc ferrite sorbents in high-temperature coal gas desulfurization, *Industrial & Engineering Chemistry Research*, 1991, 30, 100-107.
23. L.D. Gasper-Galvin, A. T. Atimatay, R.P. Gupta, Zeolite-Supported metal oxide sorbents for hot gas desulfurization, *Industrial & Engineering Chemistry Research*, 1998, 37, 4157-4166.
24. R. Ben-Slimane, M.T. Hepworth, Desulfurization of hot coal-derived fuel gases with manganese-based regenerable sorbents. 1. loading (sulfidation) test, *Energy & Fuels*, 1994a, 8, 1175-1183.

25. R. Ben-Slimane, M.T. Hepworth, Desulfurization of hot coal-derived fuel gases with manganese-based regenerable sorbents. 2. regeneration and multicycle test, *Energy & Fuels*, 1994b, 8, 1184-1191.
26. I. Barin and O. Knacke, *Thermochemical properties of inorganic substances*, Springer-Verlag, Berlin, 1973.
27. I. Barin, O. Knacke and O. Kubaschewski, *Thermochemical properties of inorganic substances, supplement*, Springer-Verlag, Berlin, 1977.
28. A.T. Altimtay, S.L. Littlefield. The use of zinc oxide sorbents to remove hydrogen sulfide from coal gases. Department of chemical engineering, Tulane university, LA.
29. Novel Technologies for gaseous contaminants control. Final report for the base program, DOE Contract No. DE-AC26-99FT40675.
30. E. Sasaoka, S. Hirano, S. Kasaoka, Y. Sakata, Characterization of reaction between zinc oxide and hydrogen sulfide, *Energy Fuels* 1994, 8(5),1100–1105.
31. K.C. Kwon et al., Reactivity of sorbents with hot hydrogen sulfide in the presence of moisture and hydrogen, *Separation Science and Technology*, 2003, 38(12-13), 3289-3311.
32. I. Novochinskii. et al., Low-Temperature H₂S removal from steam-containing gas mixtures with ZnO for fuel cell application. 1. ZnO particles and extrudates, *Energy Fuels*, 2004, 18(2), 576-583.
33. H. Fan, C.Li, H. Gao, K. Xie. Microkinetics of H₂S removal by zinc oxide in the presence of moist gas atmosphere. *Journal of natural gas chemistry*, 2003, 12, 43-48.
34. F. Huiling, L. Yanxu, L. Chunhu, G. Hanxian and X. Kechang, *Fuel Processing Technology*, 2002, 81, 91–96.
35. K. Kim, S.K. Jeon, C.Vo, Removal of hydrogen sulfide from a steam-hydrogasifier product gas by zinc oxide sorbent. *Ind. Eng.Chem.Res.* 2007,46,5848-5854.
36. H. Fan. Influence of gas composition on hydrogen sulfide removal of moderate temperature. *Bioinformatics and Biomedical Engineering, (iCBBE) 2011 5th International Conference on May 2011.*

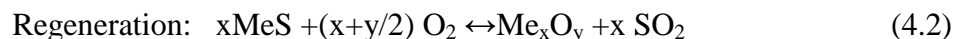
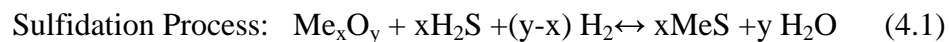
37. L. Neveux, S. Chiche, New insight on the ZnO sulfidation reaction: Evidences for an outward growth process of the ZnS phase. *Chemical Engineering Journal*. 2012(181-182), 508-515.
38. H. Fan, Y. Li, C. Li, H. Guo and K. Xie. The Apparent Kinetic of H₂S Removal by Zinc Oxide in the Presence of Hydrogen Fuel vol. 81(1), 91-6, 2002.
39. L. Li, D.L. King. H₂S removal with ZnO during fuel processing for PEMFC applications.

Chapter 4 Techno-economic Evaluation for Gas Cleanup System for CE-CERT Process

4.1 Introduction

H₂S removal by using sorbent is a much simpler, more environmentally benign process relative to scrubber technology using physical processes or chemical solvents. The only environmental concern for this process is the removal of spent sorbent. The sorbent can be categorized by regenerable sorbent and non-regenerable (disposable) sorbent. For disposable sorbent, the spent sorbent can be simply replaced with a fresh sorbent and the spent sorbent can be landfilled or, in some instances, be used as a fertilizer. For regenerable sorbent, the regeneration step can be carried out in a central location or it can be incorporated into the desulfurization process by moving the sorbent from a sulfidation reactor to a regenerable sorbents need to be able to operate through numerous sulfidation regeneration cycles with minimal loss in capacity, reactivity, and mechanical strength [1].

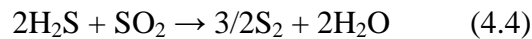
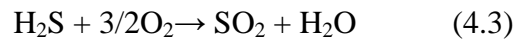
Regeneration of sorbent can be carried out by oxidation using air. The regeneration step produces SO₂ as shown below that needs to be disposed in an environmentally acceptable manner. The following reaction is observed when H₂S is reacted with a metal oxide [2]:



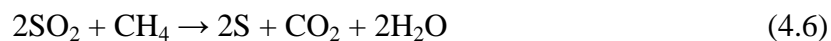
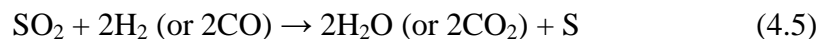
The regeneration reaction is highly exothermic requiring the use of dilute oxygen containing gas and/or some other way such as fluidized-beds to control bed temperature below the allowable temperature limit for the sorbent. A regeneration off-gas containing

SO₂ needs to be disposed in an environmentally acceptable manner [1]. There are various options for disposing the SO₂ such as conversion to elemental sulfur, or sulfuric acid. However, gasification plant sites may be far removed from sulfuric acid markets and long distance transportation is both expensive and potentially dangerous and recovery of elemental sulfur is the preferable option. A market of elemental sulfur exists, and it can be stored and transported safely at relatively low cost [2].

Two main technologies are commercially available to recover sulfur: the Claus process (partial combustion) for high levels of sulfur, and catalytic redox processes, for relatively low level of sulfur [3]. In the Claus process, roughly one-third of the H₂S is burnt to form sulfur dioxide (SO₂) (4.3). The remaining H₂S reacts with the synthesized SO₂ over an alumina or bauxite catalyst to product elemental sulfur (4.4) [4].



A catalytic redox process converts SO₂ to element sulfur by using direct sulfur recovery system (DSRP). DSRP has been developed to reduce SO₂ to elemental sulfur. The DSRP uses a stream of a reducing gas---typically a slipstream of syngas containing CO and H₂ or CH₄ in the case of coal gas desulfurization---to convert sulfur dioxide to elemental sulfur. The feed gas is at elevated temperature and pressure, and the following (simplified) reaction takes place in a gas phase, single-stage catalytic reactor [5].



For the CE-CERT process, relative low levels of H₂S can either be treated by disposable sorbent (ZnO discussed in chapter 3) or treated by regenerated ZnO based sorbent integrated with DSRP system. In this chapter, an engineering and economic evaluation for above two methods was conducted using Aspen Plus computer process simulation software.

4.1.1 Reactor and System

Several reactor configurations have been tested at the pilot-scale level using desulfurization sorbents. A transport reactor configuration was tested by M. W. Kellogg Company [6] and was installed at the Sierra Pacific Power Company (SPPCo) Pinon Pine Power plant [7]. GE Environmental Services, in conjunction with GE-CRD, tested several desulfurization sorbents for moving bed reactor applications in their fixed-bed gasifier facility. A demonstration-scale reactor was to be installed and tested at the Tampa Electric Company's (TECo) Polk Power Station I [8]. The typical reactors used in warm gas cleanup are reviewed in the next section.

4.1.1.1 Fixed-Bed Reactor

Fixed-bed reactors are the most important type of reactor for the synthesis of large scale basic chemicals and intermediates. The reaction, in these reactors, takes place in the form of a heterogeneously catalyzed gas reaction on the surface of sorbent that are arranged as a so called fixed bed in the reactor. Normally, the gas flow passing through a bed of solid particles is approximately in plug flow [2]. Conversion is close to the thermodynamic maximum. Since the sorbent particles are not transported in or out of the

reactor but fixed in a stationary bed, a fixed bed can be used for slow reactions of a gaseous component with non- or slowly deactivating solid materials. Figure 4.1 is the schematic of the fixed used for desulfurization and regeneration process [2].

The advantages of fixed-bed reactor are [2, 9]:

1. Low operation cost;
2. Continuous operation;

The disadvantages of fixed-bed reactor are:

1. Undesired thermal gradients may exist;
2. Hard to control temperature;
3. Channeling may occur;
4. Unit may be difficult to service and clean.

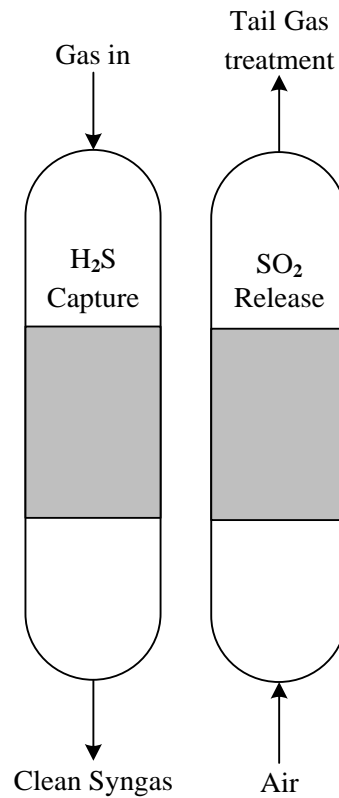


Figure 4.1 Schematic of fixed-bed reactor

4.1.1.2 Moving Bed Reactor

Moving bed is a simple form of continuous operation, see figure 4.2. It is a fixed bed of coarse solid particles which are slowly added and removed from the bed. Transport of the solids takes place by gravity, and the gas is fed either counter- or co-currently, or in cross flow with respect to the solid main-flow direction. In general, gas and solids are moving essentially in plug flow, while relatively large particles have to be applied. The maximum size is limited by the requirement of an acceptable conversion rate per unit of sorbent volume, which decreases for large particles due to the increasing effects of external and internal mass transfer limitations [2]. The minimum particle size is

determined by factors like pressure drop or, in case of counter-current operation, the risk of particle of the fluidization in the reactor. Figure 4.2 showed schematic of moving bed reactor. Regeneration and desulfurization process can be completed in one reactor [9].

The advantages of moving bed reactor are [2, 10]:

1. Easy to operate;
2. Construction cost is fairly low;
3. Scale-up is relatively simple;

The disadvantages of moving bed reactor are:

1. The particle flow is likely to be blocked (bridging);
2. Temperature control is hard, the temperature is controlled by proper gas flow or solids circulation;
3. Compared with fixed-bed, the requirement of sorbent is higher.

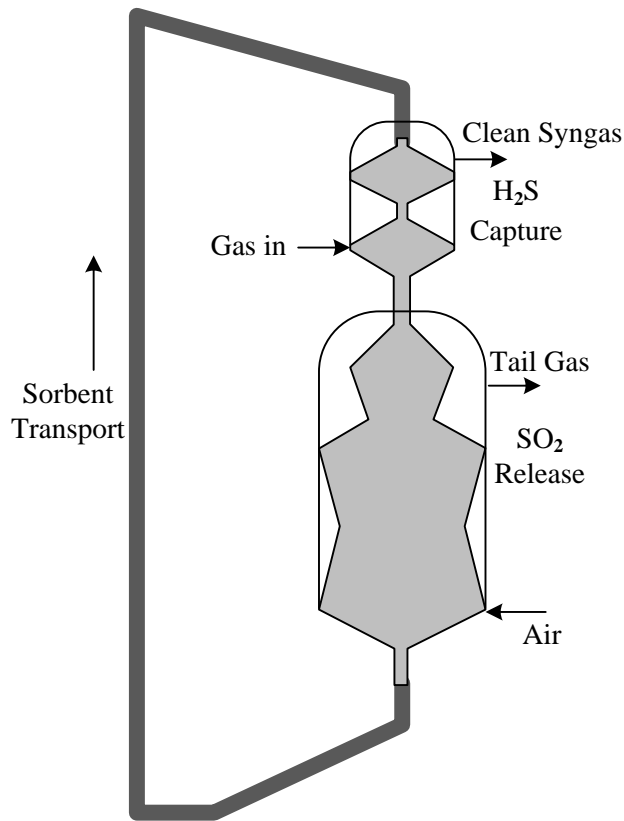


Figure 4.2 Schematic of moving-bed reactor

4.1.1.3 Fluidized Bed

In a fluidized bed, an initially stationary bed of solid particles is brought to a “fluidized” state by an upward stream of gas or liquid as soon as the volume flow rate of the fluid exceeds a certain limiting value V_{mf} (where mf denotes minimum fluidization). When the gas velocity is equal to V_{mf} , the bed begins to expand uniformly. As the gas velocity increased, solids-free gas bubbles begin to form. Ultimately, bubbles will fill the entire cross section and pass through the bed as a series of gas slugs if the bed vessel is sufficiently narrow and high. The schematic diagram of fluidized bed reactor used for warm gas cleanup system is showed in Figure 4.3 [11].

The major advantages of the (gas–solid) fluidized bed as a reaction system include [2, 12]:

1. Uniform temperature distribution due to intensive solids mixing (no hot spots even with strongly exothermic reactions);
2. High (gas-to-particle and bed-to-wall) heat and mass transfer rates;
3. Large solid-gas exchange area by virtue of small solids
4. Easy handling and transport of solids due to liquid-like behavior of the fluidized bed;

Set against these advantages are the following disadvantages:

1. Expensive solids separation or gas purification equipment required because of solids entrainment by fluidizing gas;
2. As a consequence of high solids mixing rate, non-uniform residence time of solids, back mixing of gas, and resulting lower conversion;
3. Erosion of internals and attrition of solids, resulting from high solids velocities;
4. Complex flow behavior of the gas which is divided over a bubble and an dense phase;
5. Difficulty in scaling-up.

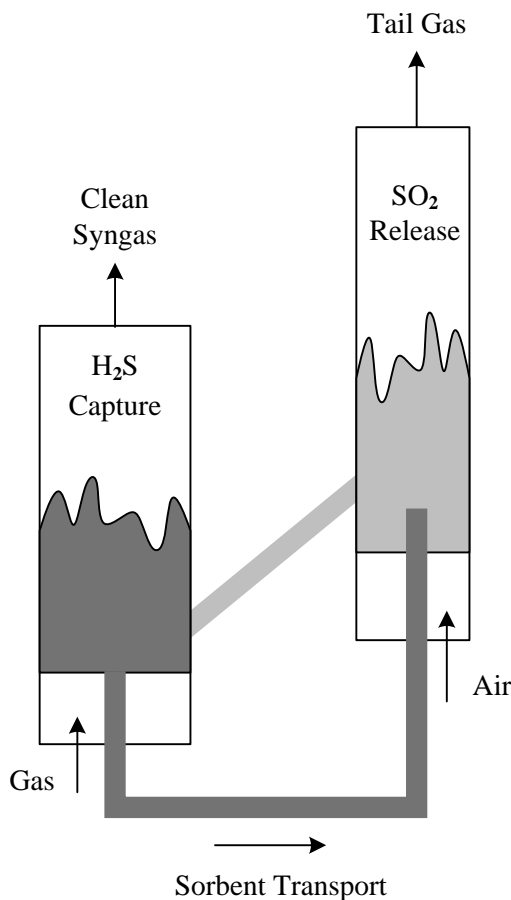


Figure 4.3 Schematic of fluidized-bed reactor

4.2 Economical Analysis of H₂S Removal by Using Regenerable Sorbent

4.2.1 Process Description

Figure 4.4 showed the H₂S removal process by using regenerable sorbent. In this process, regenerable sorbent can be regenerated by oxygen, and then recycled back to the sulfidation process. The tail gas containing SO₂ can be regenerated by H₂ to produce elemental sulfur, which separated from SMR process. The fluidized bed was chosen to be used during desulfurization and regeneration process due to several potential advantages over fixed- and moving-bed reactors, including excellent gas-solid contact, fast kinetics,

pneumatic transport, ability to handle particles in gas, and ability to control the highly exothermic regeneration process. However, an attrition-resistant sorbent that can withstand stresses induced by fluidization, transport, chemical transformation and rapid temperature swings must be developed. A mobile laboratory for DSRP demonstration with fixed-bed reactor was constructed by RTI from DOE-Morgantown gasifier, it demonstrated that, with careful control of the stoichiometric ratio of the gas input, sulfur recovery of 96% to 98% can be consistently achieved [13]. For CE-CERT process, fixed-bed reactor was chosen to be used in DSRP for recovering sulfur.

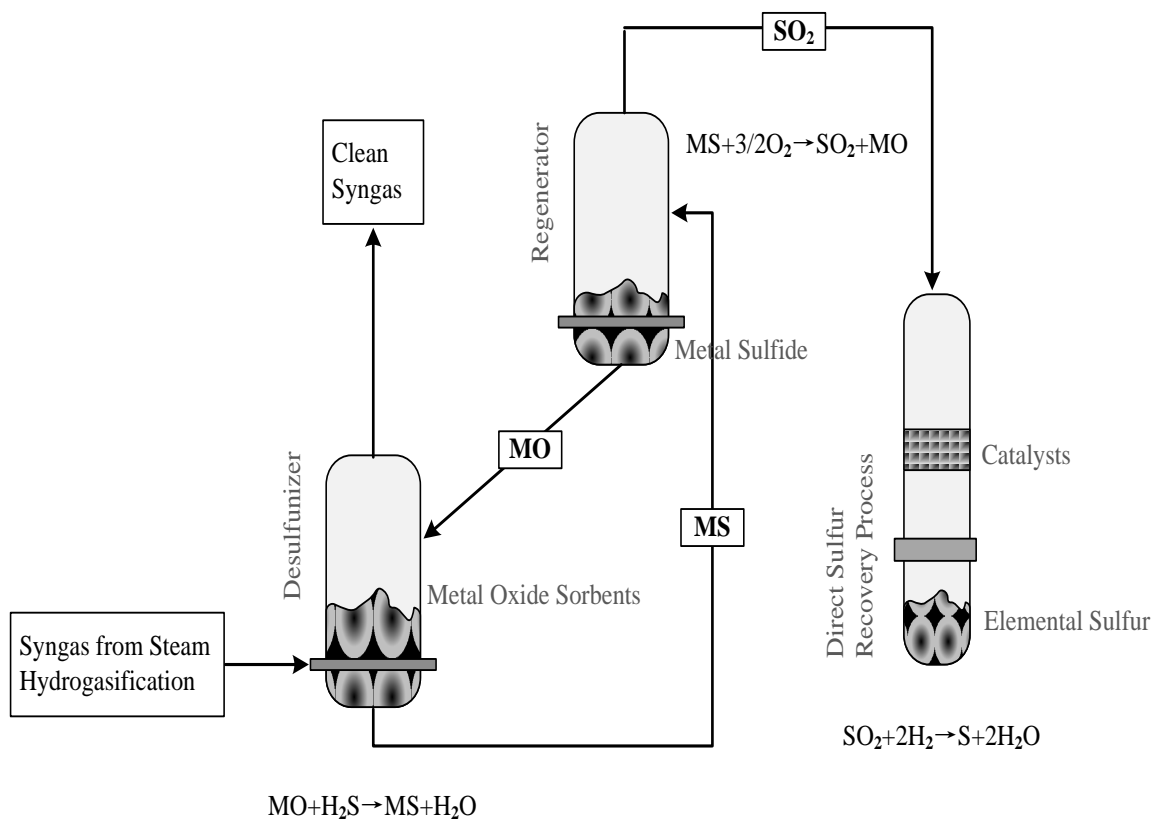
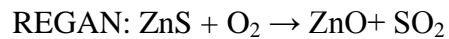
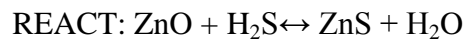


Figure 4.4 Schematic of H₂S removal process by using regenerable ZnO sorbent

4.2.2 Aspen Simulation Flow Chart

A process model using Aspen Plus has been developed according to Figure 4.4. The composition (vol %) of the input gas was 45% steam, 12.1% CH₄, 1.7% CO₂, 8.3% CO 32.9% H₂ and 1000 ppmv H₂S. This gas composition corresponds to a typical syngas generated by coal steam hydrogasification reaction. H₂S is removed from syngas in the desulfurization reactor and converted into SO₂ after regeneration process. And in the flow chart, ZnO based sorbent is used for simulation. The reaction involved in blocks in Figure 4.5 is as follows.



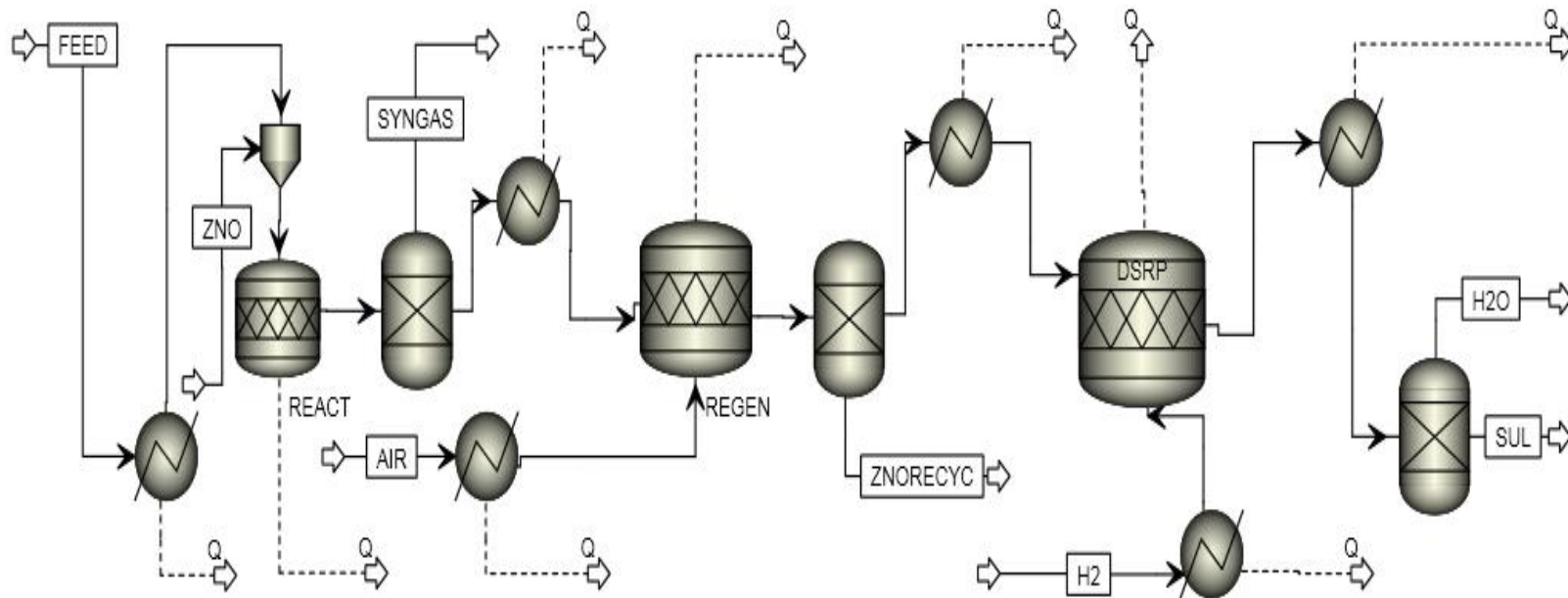


Figure 4.5 Aspen Plus simulation process flow diagram from the Aspen Plus user interface

The H₂ used for DSRP is separated from gas coming out from SMR of CE-CERT process. At the same time, ZnO produced in regeneration process will be recycled back to the desulfurization process.

Aspen Plus is utilized to organize the mass and energy streams and cost estimation software is used to generate equipment costs. Economic analysis is performed to estimate the capital investment and operating costs. However, most equipment employed in the scenarios were sized and cost estimated using Aspen Icarus Process Evaluator software. Cost for some operation units of warm gas clean up could not be evaluated by software due to their unique design and not commercial available yet. For this reason, warm gas cleanup cost was evaluated based on the report from Nexant.inc. A scaling factor α (range between 0.6-0.8) is used to scale the cost of equipment to a different size by adjusting the initial cost, Cost_o [13, 14].

$$\text{Cost}_{\text{new}} = \text{Cost}_o \times (\text{Size}_{\text{new}}/\text{Size}_o)^\alpha$$

Electricity sale price was assumed as 40 \$/Mwh and escalation factor of 2% is employed in product sale price and O&M cost to reflect inflation factor within plant lifetime. All financial values used in this paper were adjusted in 2009 dollars. A 100% Equity financing structure was assumed with 12% discount rate. Tax is not considered. A Discount Cash Flow Rate of Return (DCFROR) analysis is performed to determine the operation cost and cumulative cash flow within the plant lifetime.

4.3 Economical Analysis of H₂S Removal by Using Disposable Sorbent

4.3.1 Process Description

Figure 4.6 is the schematic diagram of desulfurization process by using fixed-bed reactor. It consists of two beds. One of the beds will be out of service at one time, being reloaded with fresh sorbent. The sorbent beds were designed to operate at an inlet temperature of 350°C. Spent sorbent removal cycle time will be about 360 days based on the assumed H₂S level in the gas stream and the sulfur capture capacity of the sorbent. At the end of the service cycle of each bed, the bed will be depressurized and cooled before removing the spent sorbent.

4.3.2 Economical Analysis

The cost of sorbent was estimated to be about \$2/kg, quotes from vendor's website. Spent sorbent was assumed to be shipped by truck to a commercial disposal site to be landfilled. With the lack of any further data at this time about the cost of sorbent landfilled. The sorbent disposal cost was estimated to be about \$0.05/kg. At the same time, due to lack of plant cost, we assumed that the cost of plant for warm gas cleanup by using disposable sorbent is 10% of that by using regenerable sorbent. The detailed information was showed in appendix.

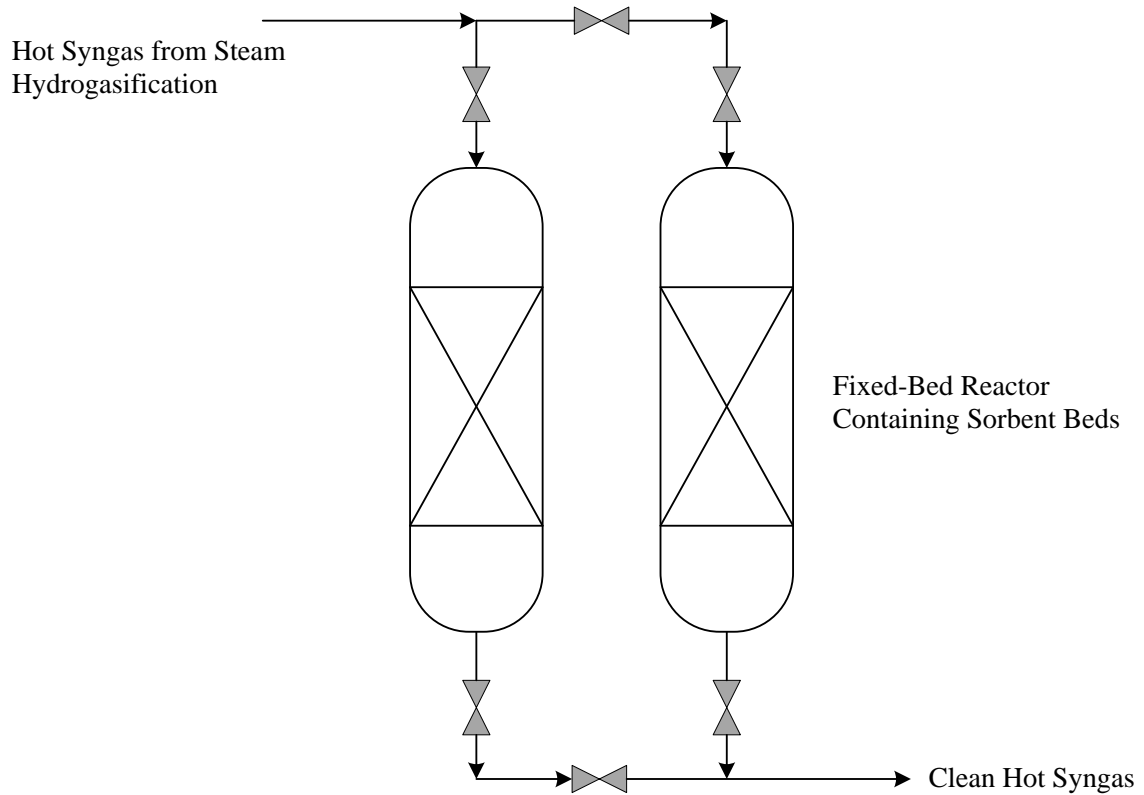


Figure 4.6 Schematic diagram of a fixed-bed reactor process for H₂S removal by using disposable sorbent

4.4. Results

4.4.1 Annual Operation Cost and Net Present Value (NPV)

According to Aspen Plus simulation results and economical analysis, the operation cost estimates for both types of using regenerable sorbents and disposable sorbents is detailed in Figure 4.7 and Figure 4.8.

The principal factors in the operating costs are sorbent related items (the cost of feed sorbent, disposable of spent sorbent), operating labor, and capital-related items. Based on the consideration of possible parameters of two different scenario (disposable

sorbent and regenerable sorbent), Figure 4.7 and Figure 4.8 showed the relationship between syngas feed and operation cost and NPV.

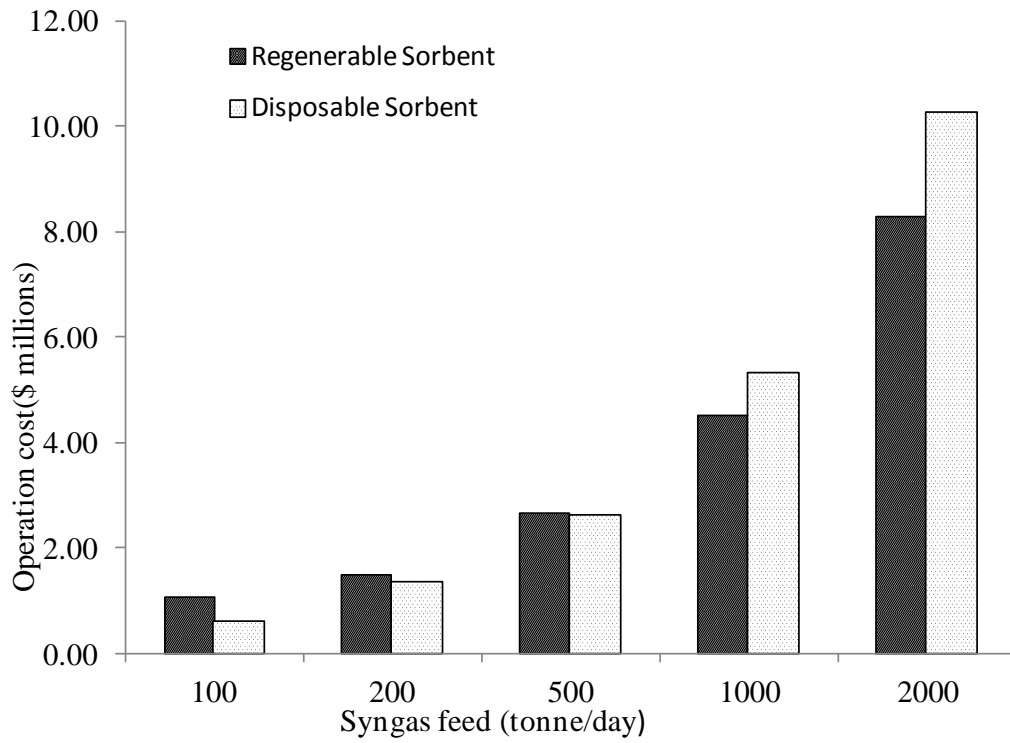


Figure 4.7 Operation cost as a function of syngas feed

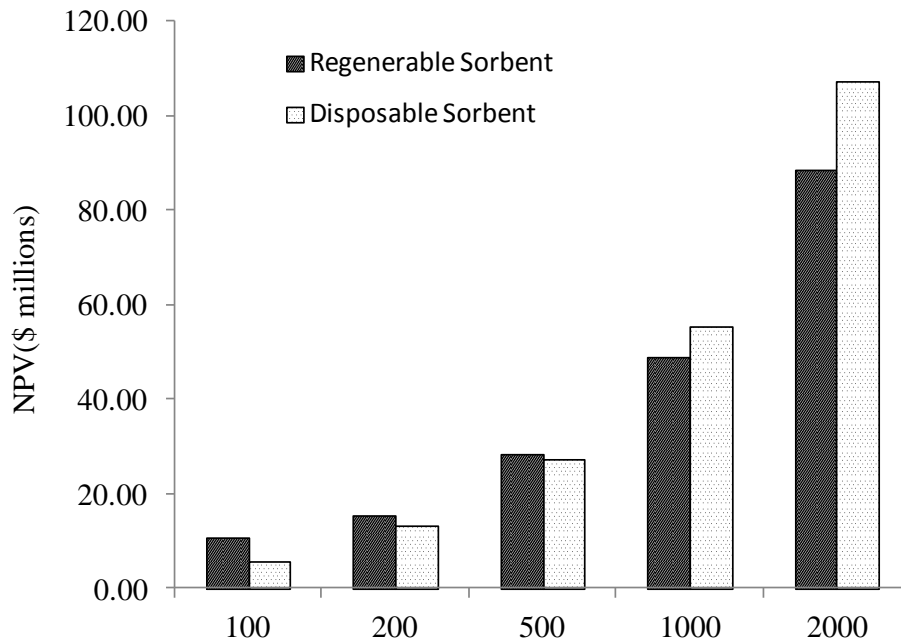


Figure 4.8 NPV as a function of syngas feed

From Figure 4.7 and 4.8, the warm gas cleanup process by using regenerable sorbent appears to be more difficult to operate and may require more employees than the warm gas cleanup process by using disposable sorbent when the syngas feed is less than 1000 tonne/day. However, with the increasing syngas feed, more elemental sulfur and more heat can be recovered during the process by using regenerable sorbents. As a result, when syngas feed is less than 1000 tonne/day, annual operating cost and NPV investment of warm gas cleanup process by using regenerable sorbent is higher than those by using disposable sorbent. While syngas feed is greater or equal than 1000 tonne/day, annual operating cost for warm gas cleanup process by using regenerable sorbent and NPV investment is considerably less than those by using disposable sorbent. Thus, warm gas cleanup process by using regenerable sorbent is feasible for high capacity plant. And

warm gas cleanup process by using disposable sorbent is more feasible for low capacity plant.

4.4.2 Economic Sensitivity Studies

A set of economic sensitivity studies was performed to test the effects of varying design and economic assumptions on the annual operation costs of the warm gas cleanup system by using regenerable sorbent and disposable sorbent when the syngas feed rate is 1000 tonne/day. Sensitivity Parameters are shown in Table 4.1 and Table 4.2 by using disposable sorbent and regenerable sorbent, respectively. The sensitivity bars are given in Figure 4.9-Figure 4.12 to demonstrate the effect of different parameter on operation cost and NPV by varying the input value within $\pm 25\%$ of baseline.

For warm gas cleanup process by using disposable sorbent (Figure 4.9 and Figure 4.10), the most influential factor is ZnO sorbent cost, since it dominates operation cost and NPV investment. The operation cost and NPV changed +22.60% and +22.57% respectively when ZnO sorbent cost increased by 25% while dropped -22.60% and -22.57% when ZnO sorbent cost decreased by 25%.

The cost of power accounts for the most important part in the operation cost and NPV For warm gas cleanup process using regenerable sorbent. Higher operation cost occurs since more H₂ is used. When power price varied $\pm 25\%$, the operation cost and NPV show a $\pm 21.29\%$ change and $\pm 16.63\%$ respectively. Fixed cost also has an important effect on the operation cost. And capital cost has the great effect on the NPV. Low sensitivity parameters include ZnO sorbent cost, sulphur cost and ZnO replaced rate.

Table 4.1 Sensitivity parameters for warm gas cleanup using disposable sorbent (syngas feed: 1000 tonne/day)

Model input	Baseline	(+25%) High Range	(-25%) Low Range
Capital Cost (\$)	1.20×10^6	1.50×10^6	9.00×10^5
ZnO Sorbent Cost (\$/kg)	2.0	2.5	1.5
Fixed Cost (\$/yr)	3.35×10^5	4.19×10^5	2.51×10^5
ZnO Disposal Cost (\$/kg)	0.050	0.0625	0.0375
Sorbent Replacement Cost (\$/time)	5.46×10^4	6.83×10^4	4.10×10^4
Sorbent Life Time (days)	360	450	270

Table 4.2 Sensitivity parameters for warm gas cleanup using regenerable sorbent (syngas feed: 1000 tonne/day)

Model input	Baseline	(+25%) High Range	(-25%) Low Range
Capital Cost (\$)	1.20×10^7	1.50×10^6	9.00×10^6
ZnO Sorbent Cost (\$/kg)	8	10	6
Fixed Cost (\$/yr)	6.70×10^5	8.38×10^5	5.03×10^5
Sulphur Price(\$/ton)	120	150	90
Steam Price(\$/lb)	0.0039	0.0049	0.0029
H ₂ equivalent price (\$/kwh)	0.04	0.05	0.03
ZnO Replaced Rate (lb/hr)	1.00	1.25	0.75

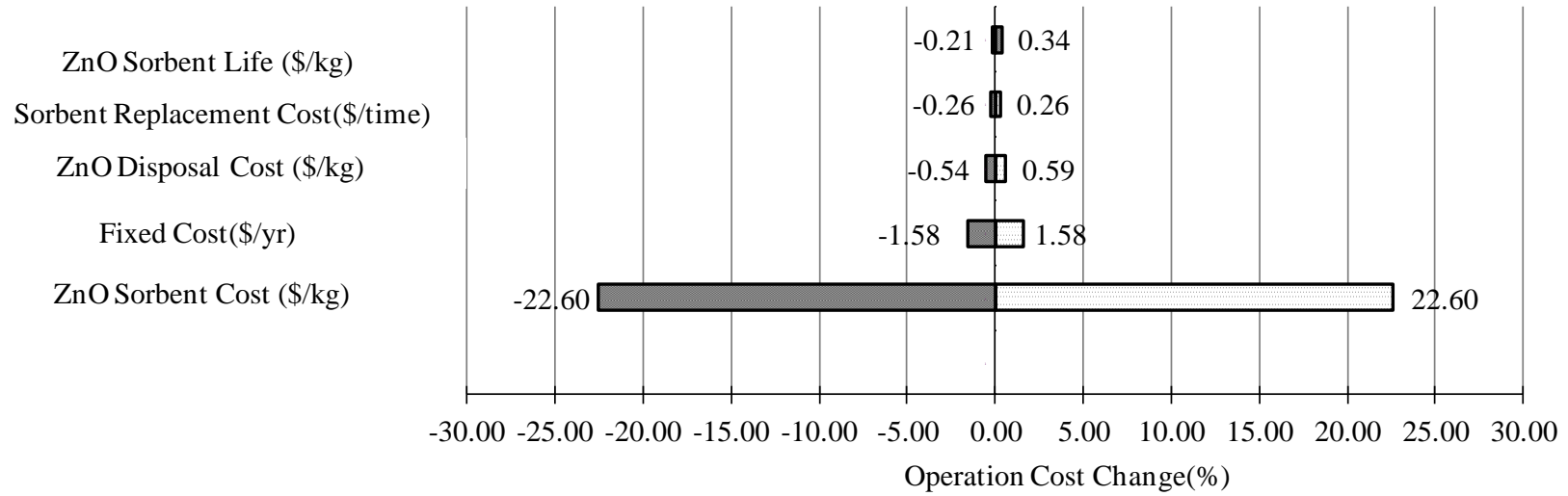


Figure 4.9 Sensitivity results for warm gas cleanup by using disposable sorbent (syngas feed rate: 1000 tonne/day)

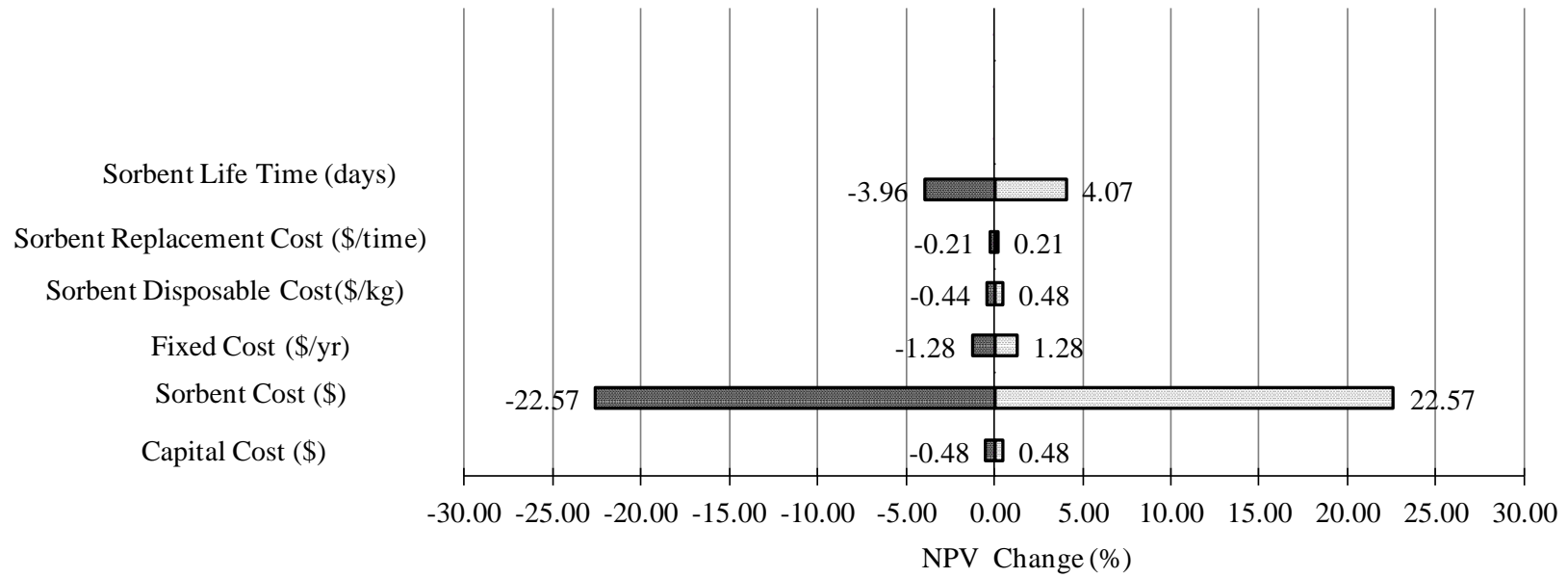


Figure 4.10 Sensitivity results for warm gas cleanup by using disposable sorbent (syngas feed rate: 1000 tonne/day)

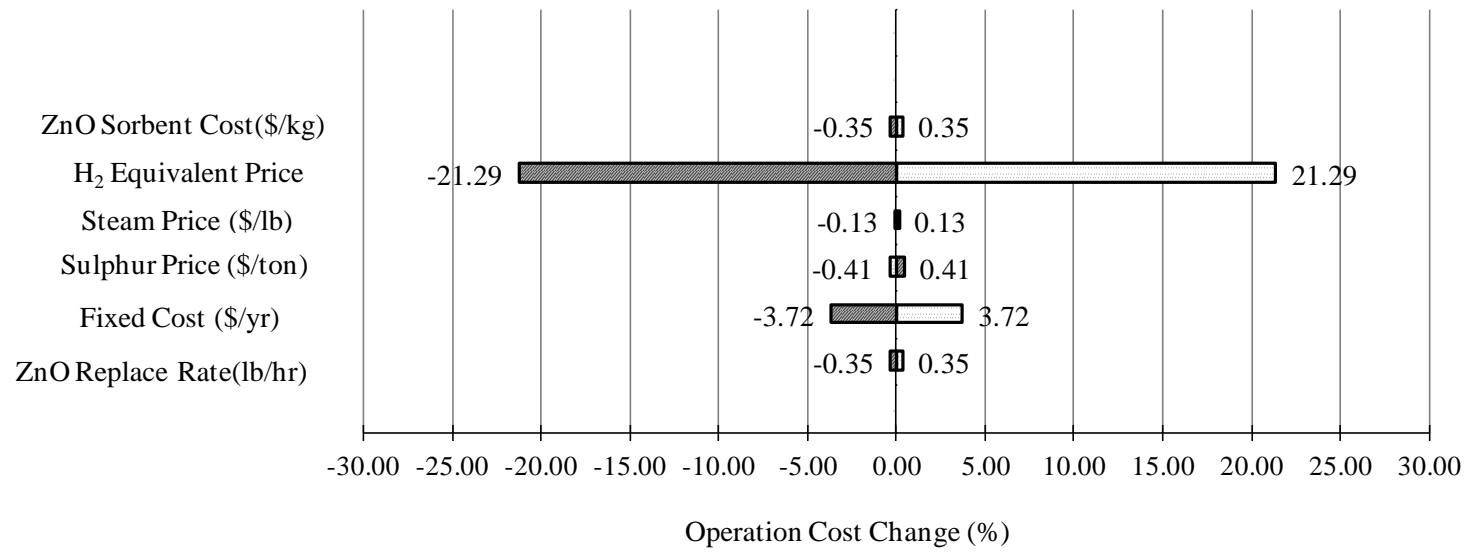


Figure 4.11 Sensitivity results for warm gas cleanup by using regenerable sorbent (syngas feed rate: 1000 tonne/day)

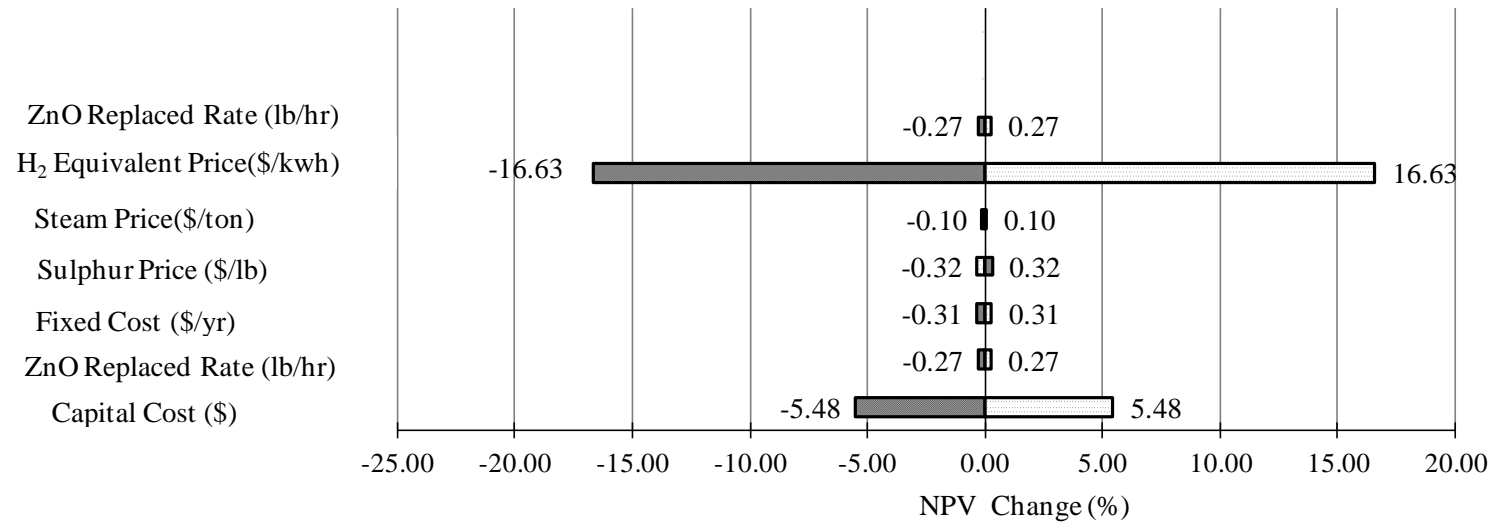


Figure 4.12 Sensitivity results for warm gas cleanup by using regenerable sorbent (syngas feed rate: 1000 tonne/day)

4.5 Conclusion

Based on Aspen simulation results and economic analysis, the following conclusions were derived:

- When syngas feed is less than 1000 tonne/day, annual operating cost and NPV investment of warm gas cleanup process by using regenerable sorbent is higher than those by using disposable sorbent. While syngas feed is greater or equal than 1000 tonne/day, annual operating cost for warm gas cleanup process by using regenerable sorbent and NPV investment is considerably less than those by using disposable sorbent.
- For warm gas cleanup process by using disposable sorbent, the most influential factor is ZnO sorbent cost. For warm gas cleanup process by using regenerable sorbent, the most important factor is the amount H₂ used in the plant.

Based on the above conclusions, the following recommendations are made:

- Warm gas cleanup process by using regenerable sorbent is feasible for high capacity plant. And warm gas cleanup process by using disposable sorbent is more feasible for low capacity plant.
- For constructing warm gas cleanup plant for CE-CERT process by using disposable sorbent, ZnO sorbent cost price should be the first problem to consider. For warm gas cleanup plant for CE-CERT process by using regenerable sorbent, the H₂ availability should be the important factor to identify.

References

1. Fuel Cells: Technologies for Fuel Processing .By James J. Spivey.
2. T. A. Aysel, P.H. Douglas, Desulfurization of hot coal gas, 1998, Berlin; New York: Springer.
3. Equipment design and cost estimation for small modular biomass systems, synthesis gas cleanup, and oxygen separation equipment
4. Techno-economic assessment of the needs for improved technology for sour oil and gas management. Eni Corporate University Scuola Enrico Mattei. Master MEDEA 2002/03.
5. G.B. Han, et al., Catalytic reduction of sulfur dioxide using hydrogen or carbon monoxide over $Ce_{1-x}Zr_xO_2$ catalysts for the recovery of elemental sulfur, Catalysis Today, 2008, 131(1-4), 330-338.
6. E. L. Moorehead, G.B. Henningsen, S. Katta, and J. J. O'Donnell, Hot gas desulfurization using transport reactors, In Proceedings of the Advanced Coal-Based Power Systems 96 Review Meeting, U.S. Department of Energy Report No.DOE/METC 96/1037, 1996.
7. J. E Demuth, and H. G. Smith, Pinon pine project gasifier startup. In proceedings of the Advanced Coal-Based Power and Environmental Systems 98 Conference, U.S. Department of Energy Report No.: DOE/FETC-98/1072, 1998.
8. R. Ayala, V.S. Venkataramani, and T. L. Chuck, Hot gas desulfurization using moving-bed reactor.” In Proceedings of the Advanced Coal-Fired Power and Environmental Systems 97 Conference, U.S. Department of Energy Report No.: DOE/METC-97/1046,1995.
9. T. Nakayama., S, Araki, E. Takahata, A. Takahashi, , Development of hot gas cleanup technology for IGCC-technical trends for 3 types hot gas cleanup process, J. Japanese Inst. of Energy, 1996, 75, 351.
10. S.K. Gangwal, Hot-gas desulfurization sorbent development for IGCC systems, in: ICHEME symp. series, 1991, 123, 59.
11. C. Eigenberger, Fixed-bed reactors. Vol, B4.
12. J. Werther, Fluidized-bed reactors, Hamburg University of Technology, Hamburg, Germany.

13. S.K. Gangwal, J.W. Portzer, Bench-scale demonstration of hot-gas desulfurization technology. Topical report. Contract no: DE-AC21-93MC30010.
14. Preliminary feasibility analysis of RTI warm gas cleanup(WGCU) technology, Nexant.
15. R.M. Swanson, J.A. Satrio, R.C. Brown. Techno-economic analysis of biofuels production based on gasification. National renewable energy laboratory.

Chapter 5 Conclusions and Future Work

This section summarized the conclusions derived from experimental and simulation work performed as part of this thesis. Three sub tasks were completed with the following conclusions:

1. A series of experiments have been performed using a stirred batch reactor to investigate the formation of gaseous sulfur species in steam hydrogasification reaction. In this task, the following results were obtained:
 - In the steam hydrogasification reaction with coal as the feedstock, H_2S is the only sulfur containing species detected in the gas phase. Such results is promising, Not only because COS and CS_2 are more difficult to remove compared with H_2S , but also because carbon is wasted if it was converted into COS and CS_2 . Elimination both COS and CS_2 will increase the potential of the carbon conversion to synthesis gas.
 - The formation of H_2S increased with increasing temperature in the reactor, which can be explained as more sulfur leaving the solid matrix of coal with higher temperatures. At the same time, H_2S release increased when the water to coal mass ratio increased. The possible reason for this is that steam reacts with pyrite promoting the formation of H_2S .
 - H_2S was reduced with increasing H_2 partial pressure. It is speculated that H_2S produced by decomposition of pyrite will be captured by the organic matrix at the higher H_2 partial pressure.

2. A lab-scale warm gas cleanup system was developed to remove H₂S from syngas, whose composition based on the experimental result with the typical condition in the experiment of task one. The ability of zinc oxide sorbent to removal H₂S was examined as a function of space velocity and gas composition. In this task, the following results were concluded:
 - Sulfur capture capacity of sorbent and H₂S breakthrough time increased with decreasing space velocity, which was the result of longer contact time between gas H₂S and solid ZnO.
 - Addition of H₂ or CH₄ to the inlet wet gas stream increased the breakthrough time, which is likely to be related with the adsorption behavior of H₂ and CH₄ on ZnO surface, which could enhance the basicity of the ZnO surface.
 - Addition of CO to the inlet wet gas stream has the negative effect on breakthrough time, as a result of carbon deposition on the surface of ZnO, which hindered the reaction between ZnO and H₂S. Adding lower content of CO₂ in the inlet wet gas stream almost have no influence on the H₂S breakthrough time.
 - Addition of mixture gas containing CO, CO₂, CH₄ and H₂ into inlet gas has a positive effect on breakthrough time.
3. A techno-economic analysis was completed based Aspen simulation results and economic analysis to design warm gas cleanup system for CE-CERT process. In this task, the following results were concluded:

- Annual operation cost and NPV investment of warm gas cleanup process by using disposable sorbent is lower than those by using regenerable sorbent when the syngas feed rate is less than 1000 tonne/day. While annual operation cost and NPV investment of warm gas cleanup process by using disposable sorbent is considerable higher than those by using regenerable sorbent when the syngas feed is greater or equal than 1000 tonne/day.
- For warm gas cleanup process by using regenerable sorbent, the most influential factor of economic sensitivity analysis is the availability of H₂ used in the plant. The most influential factor using a warm gas cleanup process using disposable sorbents is the cost of ZnO sorbent.

Appendices

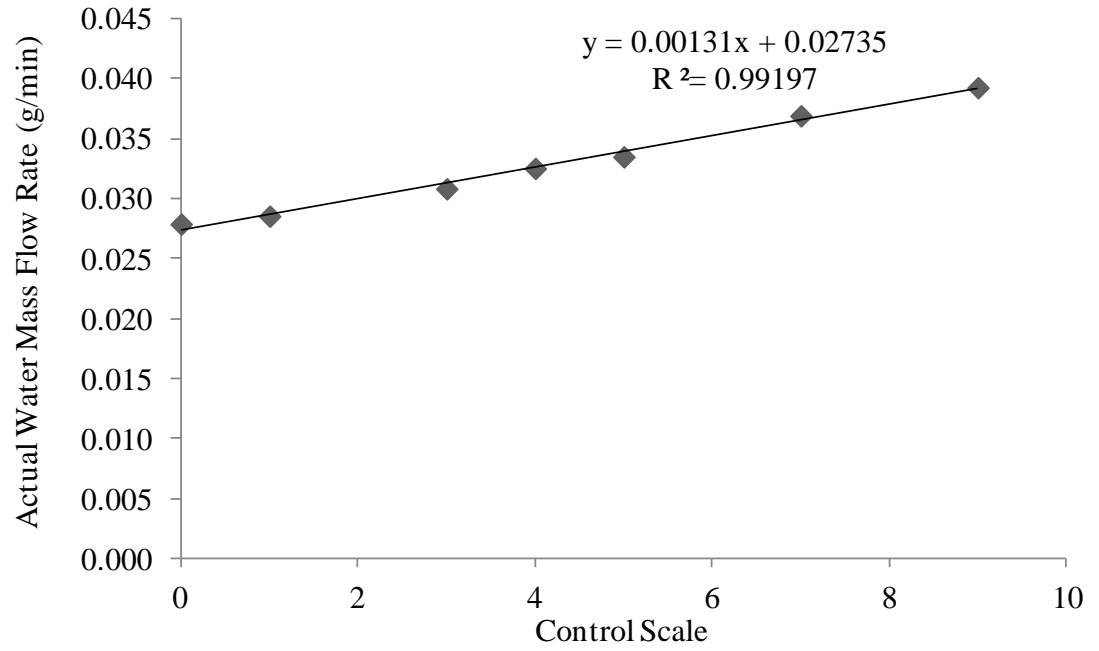


Figure 1 Calibration curve of water pump

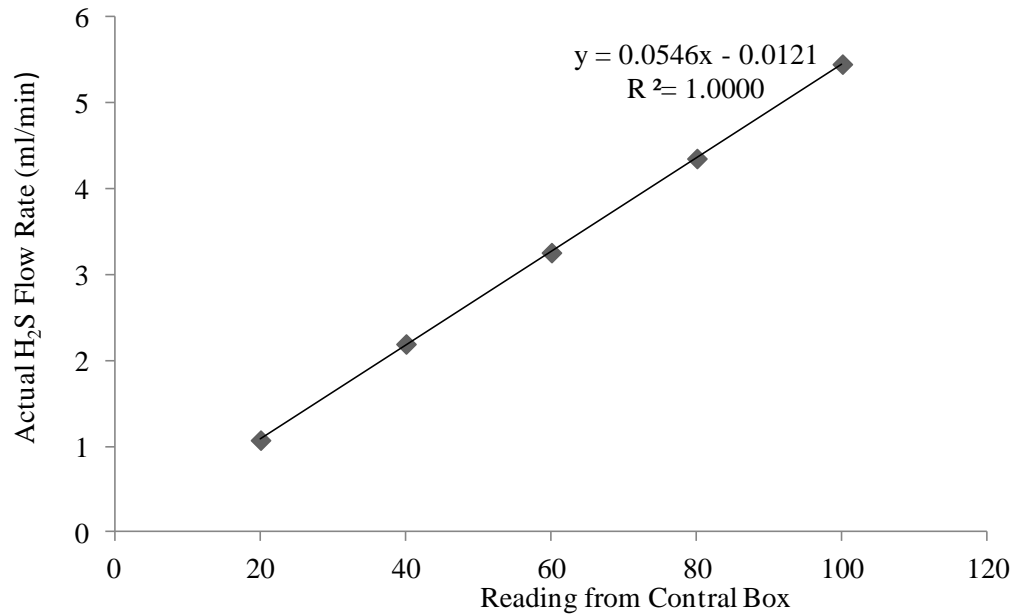


Figure 2 Calibration curve of H₂S mass flow controller